Conversion of a Diruthenium μ-Methylene Complex, $Cp_2Ru_2(\mu\text{-}CH_2)(\mu\text{-}CO)(CO)_2$, into Methane through Reduction with Hydrosilane: Reactivity of Silyl−μ-Methylene Intermediates $Cp_2Ru_2(\mu\text{-}CH_2)(SiR_3)(X)(CO)_2$ (X = H, SiR_3) Relevant to Catalytic CO Hydrogenation and Activation of Si−H, C−H, and C−Si Bonds

Munetaka Akita,* Ruimao Hua, Tomoharu Oku, Masako Tanaka, and Yoshihiko Moro-oka*

Research Laboratory of Resources Utilization, Tokyo Institute of Technology, 4259 Nagatsuta, Midori-ku, Yokohama 226, Japan

Received April 4, 1996[⊗]

Thermolysis (170 °C, 3 days) of a diruthenium μ-methylene complex, $Cp_2Ru_2(\mu\text{-}CH_2)(\mu\text{-}CO)(CO)_2$ (**1**), in the presence of $HSiMe_3$ produces methane along with methylsilane ($SiMe_4$) and mononuclear organometallic products, $CpRu(H)(SiR_3)_2(CO)$ (**2**) and $CpRu(CO)_2(SiMe_3)$ (**3**). The reaction mechanism involving initial CO dissociation has been investigated by using a labile μ-methylene species, $Cp_2Ru_2(\mu\text{-}CH_2)(\mu\text{-}CO)(CO)(MeCN)$ (**4**), the MeCN adduct of the coordinatively unsaturated species resulting from decarbonylation of **1**. Treatment of **4** with $HSiR_3$ produces the hydrido−silyl−μ-methylene intermediate $Cp_2Ru_2(\mu\text{-}CH_2)(H)(SiR_3)(CO)_2$ (**5**) and the disilyl−μ-methylene complex $Cp_2Ru_2(\mu\text{-}CH_2)(SiR_3)_2(CO)_2$ (**6**) successively. Further reaction of **5** and **6** with $HSiR_3$ affords methane under milder conditions (120 °C, 12 h) compared to the methane formation from **1**. Meanwhile complicated exchange processes are observed for the silylated μ-methylene species **5** and **6**. The dynamic behavior of the hydrido−silyl species **5** giving a ^{1}H-NMR spectrum consistent with an apparent C_s structure at ambient temperature has been analyzed in terms of a mechanism involving intramolecular H- and R_3Si-group migration between the two ruthenium centers. It is also revealed that intramolecular exchange reaction of the hydride and μ-CH_2 atoms in **5** proceeds via the coordinatively unsaturated methyl intermediate $Cp_2Ru_2(CH_3)(SiR_3)(CO)_2$ (**9**). In addition to these intramolecular processes, the hydride, μ-CH_2, and SiR_3 groups in **5** and **6** exchange with external $HSiR_3$ via replacement of the η^2-bonded H_2 or $HSiR_3$ ligand in μ-methylene or μ-silylmethylene intermediates $Cp_2Ru_2(\mu\text{-}CHX)(\mu\text{-}CO)(CO)(\eta^2\text{-}H\text{-}Y)$ [X, Y = H, SiR_3 (**7**), SiR_3, H (**18**), SiR_3, SiR_3 (**16**)] as confirmed by trapping experiments of **7** with L (CO, PPh_3) giving $Cp_2Ru_2(\mu\text{-}CHX)(\mu\text{-}CO)(CO)(L)$ [X, L = H, CO (**1**), H, PPh_3 (**11**), SiR_3, CO (**12**), SiR_3, PPh_3 (**13**)]. Hydrostannanes ($HSnR_3$) also react with **4**, in a manner similar to the reaction with $HSiR_3$, to give the hydrido−stannyl−μ-methylene intermediate $Cp_2Ru_2(\mu\text{-}CH_2)(H)(SnR_3)(CO)_2$ (**20**) and the distannyl−μ-methylene complex $Cp_2Ru_2(\mu\text{-}CH_2)(SnR_3)_2(CO)_2$ (**21**) successively (the stannyl analogues of **5** and **6**, respectively). The intramolecular exchange processes (H ↔ SnR_3, H ↔ μ-CH_2) are also observed for **20**. But the $HSnPh_3$ adduct **20c** is further converted to a mixture containing the μ-η^1:η^2-phenyl complex $Cp_2Ru_2(\mu\text{-}Ph)(SnCH_3Ph_2)(CO)_2$ (**22**) and the bis(μ-stannylene) complex $Cp_2Ru_2(\mu\text{-}SnPh_2)_2(CO)_2$ (**23**) instead of **21c**. The isolation of **22** supports viability of the methyl species (**9**). These results suggest that methane formation from **1** follows (i) CO dissociation, (ii) H−SiR_3 oxidative addition giving the hydrido−silyl−μ-methylene intermediate **5**, (iii) equilibrium with the methyl intermediate **9**, (iv) a second oxidative addition of H−SiR_3, and (v) elimination of methane repeating reductive elimination from mono- and dinuclear hydrido−methyl intermediates **27** and **28**. The present reaction sequence can be viewed as a model system for methanation via the Fischer−Tropsch mechanism where hydrosilane behaves as a H_2 equivalent (pseudo-hydrogen). The molecular structures of **6d**,**e**, **12a**, **13a**, **21a**, and **22** have been determined by X-ray crystallography.

Introduction

Polynuclear transition metal complexes containing a bridging methylene (alkylidene) ligand[1] have been investigated as model compounds for surface-bound methylene species, which should play a pivotal role in surface-catalyzed transformations of carbon monoxide

(1) (a) Herrmann, W. A. *Adv. Organomet. Chem.* **1982**, *20*, 159. (b) Herrmann, W. A. *J. Organomet. Chem.* **1983**, *250*, 319. (c) Saez, I. M.; Andrews, D. G.; Maitlis, P. M. *Polyhedron* **1988**, *7*, 827. (d) Puddephatt, R. J. *Polyhedron* **1988**, *7*, 767. (e) Knox, S. A. R. *J. Organomet. Chem.* **1990**, *400*, 255.

[⊗] Abstract published in *Advance ACS Abstracts,* August 15, 1996.

S0276-7333(96)00258-0 CCC: $12.00

Scheme 1

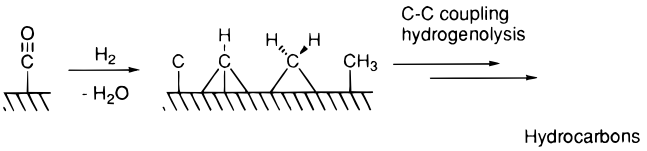

and hydrocarbons (Scheme 1).[2,3] Extensive studies on their reactivity with emphasis on coupling with hydrocarbyl species (e.g. another methylene ligand present in the complex and external alkenes and alkynes) have provided us with suggestive information on the mechanism of the carbon-chain propagation step of catalytic CO hydrogenation.[4] In connection with the present study, various aspects of $Cp_2Ru_2(\mu\text{-}CR_2)(\mu\text{-CO or } CR_2)\text{-}(CO)_2$-type diruthenium bridging alkylidene complexes have been scrutinized by Knox and his co-workers.[5] Meanwhile hydrogenation or protonation of a hydrocarbyl species releasing hydrocarbons serve as a model system for the termination step.

Reduction of organometallic compounds by using hydrosilane as a H_2 equivalent has been a subject of our research.[6] Because the reaction features of the H−Si bond in hydrosilanes are quite similar to those of the H−H bond in dihydrogen [e.g. oxidative addition to a low-valent metal center and catalyzed addition reactions to unsaturated organic compounds (hydrogenation vs hydrosilation)], hydrosilane can be considered as a pseudo-hydrogen. In addition to these features, the oxygenophilic Si part induces Lewis acidic activation of oxygen-containing functional groups to promote hydride transfer leading to the formation of hydrocarbyl species after removal of the oxygen atom.[7] Thus employment of hydrosilane as a H_2 equivalent would lead to successful modeling of two types of reduction steps, i.e. (i) deoxygenative reduction of O-containing functional groups and (ii) hydrogenolysis of M−C bonds.

Scheme 2

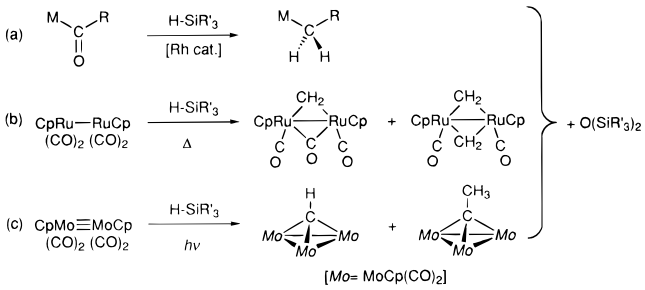

Scheme 3

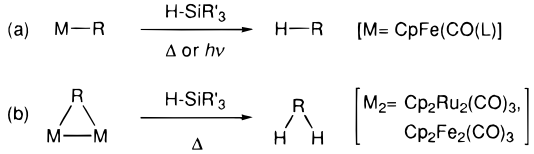

In previous papers we reported deoxygenative reduction of acyl and carbonyl ligands giving alkyl, methylene, and alkylidyne species accompanied by elimination of siloxane (Scheme 2).[6a,c,e,g,i] These ligand transformations may be viewed as model systems for formation step of hydrocarbyl intermediates in Fischer−Tropsch and Pichler−Schulz mechanisms. We also reported reduction of alkyliron complexes $[CpFe(CO)_2R]$ with hydrosilane producing alkane (R−H), a formal hydrogenolysis product (reaction a in Scheme 3).[6b,d] As an extension, we have studied reduction of a dinuclear complex with a difunctional hydrocarbyl ligand. Herein we disclose details of conversion of a μ-methylene complex of ruthenium, $Cp_2Ru_2(\mu\text{-}CH_2)(\mu\text{-CO})(CO)_2$, into methane by treatment with hydrosilanes (reaction b in Scheme 3).[8] Employment of $HSiR_3$ leads to successful isolation and characterization of intermediates which are stabilized by Ru−Si interactions. Furthermore combination of the present M−C bond hydrogenolysis with the previously reported deoxygenative reduction of $Cp_2Ru_2(CO)_4$ (reaction b in Scheme 2)[6f] would lead to a model system for methanation.

Results and Discussion

Conversion of the μ-Methylene Ligand in $Cp_2Ru_2(\mu\text{-}CH_2)(\mu\text{-CO})(CO)_2$ (1) into Methane. Treatment of

(2) (a) Masters, C. *Adv. Organomet. Chem.* **1979**, *19*, 63. (b) Muetterties, E. L.; Rhodin, T. N.; Band, E.; Brucker, C. F.; Pretzer, W. R. *Chem. Rev.* **1979**, *79*, 79. (c) Roofer-DePoorter, C. K. *Chem. Rev.* **1981**, *81*, 447. (d) Herrmann, W. A. *Angew. Chem., Int. Ed. Engl.* **1982**, *21*, 117. (e) Cutler, A. R.; Hanna, P. K.; Vites, J. C. *Chem. Rev.* **1988**, *88*, 1363 and references cited therein. For carbide complexes: (f) Tachikawa, M.; Muetterties, E. L. *Prog. Inorg. Chem.* **1981**, *28*, 203. (g) Bradley, J. S. *Adv. Organomet. Chem.* **1983**, *22*, 1. (h) Shriver, D. F.; Sailor, M. J. *Acc. Chem. Res.* **1988**, *21*, 374. See also: (i) Beck, W.; Niemer, B.; Wieser, M. *Angew. Chem., Int. Ed. Engl.* **1993**, *32*, 923.

(3) (a) Falbe, J. *New Synthesis with Carbon Monoxide*; Springer: Berlin, 1980. (b) Keim, W. *Catalysis in C1 Chemistry*; D. Reidel: Dordrecht, The Netherlands, 1983. (c) Anderson, R. B. *The Fischer−Tropsch Synthesis*; Academic Press: London, 1984. (d) Pines, H. *The Chemistry of Catalytic Hydrocarbon Conversions*; Academic Press: London, 1981. (e) Somorjai, G. A. *Introduction to Surface Chemistry and Catalysis*; John Wiley & Sons: New York, 1994.

(4) See, for example: Maitlis, P. M. *J. Organomet. Chem.* **1995**, *500*, 239 and references cited therein.

(5) (a) Dyke, A. F.; Knox, S. A. R.; Morris, M. J.; Naish, P. J. *J. Chem. Soc., Dalton Trans.* **1983**, 1417. (b) Colborn, R. E.; Dyke, A. F.; Knox, S. A. R.; Mead, K.; Woodward, P. *J. Chem. Soc., Dalton Trans.* **1983**, 2099. (c) Colborn, R. E.; Davies, D. L.; Dyke, A. F.; Endesfelder, A.; Knox, S. A. R.; Orpen, A. G., Plaas, D *J. Chem. Soc., Dalton Trans.* **1983**, 2661. (d) Adams, P. Q.; Davies, D. L.; Dyke, A. F.; Knox, S. A. R.; Mead, K.; Woodward, P *J. Chem. Soc., Chem. Commun.* **1983**, 222. (e) Forrow, N. J.; Knox, S. A. R.; Morris, M. J.; Orpen, A. G. *J. Chem. Soc., Chem. Commun.* **1983**, 234. (f) Davies, D. L.; Knox, S. A. R.; Mead, K. A.; Morris, M. J.; Woodward, P *J. Chem. Soc., Dalton Trans.* **1984**, 2293. (g) Davies, D. L.; Gracey, B. P.; Guerchais, V.; Dyke, A. F.; Knox, S. A. R.; Orpen, A. G. *J. Chem. Soc., Chem. Commun.* **1984**, 841. (h) Connelly, N. G.; Forrow, N. J.; Gracey, B. P.; Knox, S. A. R.; Orpen, A. G. *J. Chem. Soc., Chem. Commun.* **1985**, 14. (i) Colborn, R. E.; Davies, D. L.; Dyke, A. F.; Knox, S. A. R.; Mead, K.; Orpen, A. G. *J. Chem. Soc., Dalton Trans.* **1989**, 1799. (j) Doherty, N. M.; Howard, J. A.; Knox, S. A. R.; Terril, N. J.; Yates, M. I. *J. Chem. Soc., Chem. Commun.* **1989**, 638. (k) Howard, J. A.; Knox, S. A. R.; Terril, N. J.; Yates, M. I. *J. Chem. Soc., Chem. Commun.* **1989**, 640. (l) Fildes. M. J.; Knox, S. A. R.; Orpen, A. G.; Turner, M. L.; Yates, M. I. *J. Chem. Soc., Chem. Commun.* **1989**, 1680. See also the following review articles: (m) Knox, S. A. R. *J. Organomet. Chem.* **1990**, *400*, 255. (n) Knox, S. A. R. *J. Cluster Sci.* **1992**, *3*, 385.

(6) (a) Akita, M.; Mitani, O.; Moro-oka, Y. *J. Chem. Soc., Chem. Commun.* **1989**, 527. (b) Akita, M.; Oku, T.; Moro-oka, Y. *J. Chem. Soc., Chem. Commun.* **1990**, 1790. (c) Akita, M.; Mitani, O.; Sayama, M.; Moro-oka, Y. *Organometallics* **1991**, *10*, 1394. (d) Akita, M.; Oku, T.; Tanaka, M.; Moro-oka, Y. *Organometallics* **1991**, *10*, 3080. (e) Akita, M.; Oku, T.; Moro-oka, Y. *J. Chem. Soc., Chem. Commun.* **1992**, 1031. (f) Akita, M.; Oku, T.; Hua, R.; Moro-oka, Y. *J. Chem. Soc., Chem. Commun.* **1993**, 1670. (g) Akita, M.; Noda, K.; Moro-oka, Y. *Organometallics* **1994**, *13*, 4145. (h) Akita, M.; Moro-oka, Y. *Stud. Surf. Sci. Catal.* **1995**, *92*, 137. (i) Akita, M.; Noda, K.; Takahashi, Y.; Moro-oka, Y. *Organometallics* **1995**, *14*, 5209. (j) Akita, M.; Hua, R.; Oku, T.; Moro-oka, Y. *Organometallics* **1996**, *15*, 2548. (k) Akita, M.; Hua, R.; Oku, T.; Moro-oka, Y. *J. Chem. Soc., Chem. Commun.* **1996**, 541.

(7) (a) *The chemistry of organosilicon compounds*; Patai, S., Rappoport, Z., Eds.; John Wiley & Sons: Chichester, U.K., **1989**; Vols. 1 and 2. (b) *Comprehensive Organometallic Chemistry I and II*; Abel, E. W., Stone, F. G. A., Wilkinson, G., Eds.; Pergamon: Oxford, 1982 and 1995. (c) Colvin, E. W. *Silicon in Organic Synthesis*; Butterworths: London, 1981; Chapter 21. (d) Weber, W. P. *Silicon Reagents for Organic Synthesis*; Springer: Berlin; 1983; Chapter 17.

(8) A preliminary account of the present result was already reported in communications. See refs 6f,k.

a toluene solution of the diruthenium μ-methylene complex **1** with monohydrosilane at 170 °C (in a sealed tube) produced a mixture of methane and methylsilane together with mononuclear Ru complexes, $CpRu(H)(SiR_3)_2(CO)$ (**2**) and $CpRu(CO)_2$-$SiMe_3$ (**3**)[9] (eq 1). In

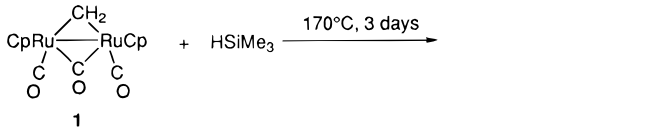

CH_4 (42 %) + CH_3-$SiMe_3$ (18 %) (1)
+ $CpRu(H)(SiMe_3)_2(CO)$ (**2**: 9 %)
+ $CpRu(CO)_2$-$SiMe_3$ (**3**: 22 %)

contrast to the reaction with monohydrosilane, reaction with di- or trihydrosilanes resulted in reduction of the μ-CO ligand to give the di(μ-methylene) complex, $Cp_2Ru_2(\mu\text{-}CH_2)_2(CO)_2$, as we reported previously.[6e,j,10]

Because the reaction conditions are much more vigorous compared to those of the alkane formation from the alkyliron complexes induced by hydrosilane [M = $FeCp(CO)_2$ (90 °C, 10 h); Scheme 3a], it is suggested that the initial step may involve a CO-dissociation process, though some other mechanisms via coordinatively unsaturated intermediates arising from, for example, Cp slippage (an η^3-Cp intermediate)[11] and CO insertion (a μ-ketene species)[12] are possible.

Reaction of $Cp_2Ru_2(\mu\text{-}CH_2)(\mu\text{-}CO)(CO)(MeCN)$ (4) with Hydrosilanes Leading to Silylated μ-Methylene Species $Cp_2Ru_2(\mu\text{-}CH_2)(X)(SiR_3)(CO)$ [5 (X = H), 6 (X = SiR_3)]. In order to investigate participation of initial CO dissociation, we examined reactivity of the labile MeCN adduct (**4**)[5j] of the coordinatively unsaturated species "$Cp_2Ru_2(\mu\text{-}CH_2)(\mu\text{-}CO)(CO)$"[13] arising from decarbonylation of **1** (Scheme 4). As a result, **4** readily reacted with hydrosilane at ambient temperature to give hydrido−silyl−μ-methylene $Cp_2Ru_2(\mu\text{-}CH_2)(H)(SiR_3)(CO)_2$ (**5**) and disilyl−μ-methylene species $Cp_2Ru_2(\mu\text{-}CH_2)(SiR_3)_2(CO)_2$ (**6**) successively. Further heating of these μ-methylene complexes **5** and **6** at 120 °C in the presence of excess $HSiMe_3$ produced methane (eq 2). It

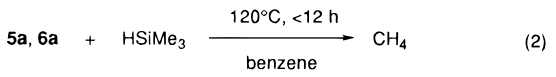

is notable that the reaction conditions for the methane formation (120 °C, <12 h) were much milder than those of eq 1 (170 °C, 3 days). Thus we have concluded that (i) the methane formation is initiated by rate-determining CO dissociation and (ii) it involves the silylated μ-methylene species **5** and **6** as reaction intermediates. Similar hydrocarbon elimination from a dinuclear bridging hydrocarbyl complex was reported by Casey et al.[14] Photochemical reduction of a diiron μ-vinylidene complex $Cp_2Fe_2(\mu\text{-}C{=}CH_2)(\mu\text{-}CO)(CO)_2$ with H_2 and $HSiMe_3$ produced ethylene and vinylsilane $CH_2{=}CH{-}SiMe_3$, respectively. Initial generation of a coordinatively unsaturated intermediate was proposed to be a key step on the basis of a ^{13}CO-incorporation experiment.

Scheme 4

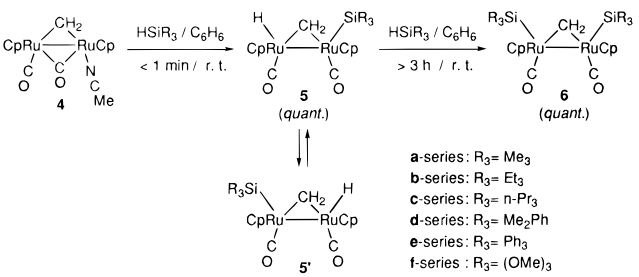

Scheme 5

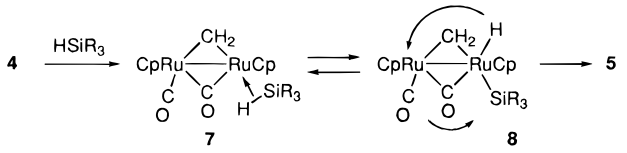

From the next section each step of Scheme 4 is discussed in detail.

(i) Formation and Characterization of Hydrido−Silyl−μ-Methylene (5) and Disilyl−μ-Methylene Species (6). Addition of hydrosilane to a benzene or toluene suspension of **4** caused immediate dissolution of the solid to give a homogeneous solution of the hydrido−silyl−μ-methylene species **5** in a quantitative yield (Scheme 4). When the mixture was left for a prolonged time (>3 h) at ambient temperature or heated for 15 min at 55 °C, **5** was gradually converted to the disilyl−μ-methylene complex **6** quantitatively with evolution of H_2.[15] (For complete conversion to **6** it was requisite to stir a mixture overnight, when the reaction was carried out at rt (room temperature)).

Formation of the hydrido−silyl−μ-methylene species **5** may follow the following reaction sequence: (i) displacement of the labile MeCN ligand by hydrosilane giving the η^2-bonded intermediate **7**; (ii) oxidative addition of the H−Si bond leading to the hydrido−silyl species **8**; (iii) intramolecular migration of the H (or SiR_3) and μ-CO ligands (Scheme 5).

Because compounds **5** could not be isolated in a pure form owing to thermal instability resulting in the formation of **6**, they were characterized spectroscopically (Table 1). Although **5** shows dynamic behavior as described below, the ^{1}H-NMR spectrum of **5a** observed at −60 °C contains the hydride and $SiMe_3$ signals in addition to the μ-CH_2 and two Cp signals (Figure 1). The lack of a μ-CO vibration and comparison with **6** (see below) lead to the assignment to the structure depicted in Scheme 4, which is also consistent with the ^{13}C-NMR data. While both of *cis*- and *trans*-structures are possible for **5**, the configuration cannot be determined by means of spectroscopic data alone.

(9) Sosinsky, B. A.; Knox, S. A. R.; Stone, F. G. A. *J. Chem. Soc., Dalton Trans.* **1975**, 1633.

(10) Thermal reaction with $HSnMe_3$ was also attempted, but $HSnMe_3$ decomposed under the reaction conditions.

(11) Casey, C. P.; O'Conner, J. M. *Chem. Rev.* **1987**, *87*, 307.

(12) (a) Lin, Y. C.; Calabrese, J. C.; Wreford, S. S. *J. Am. Chem. Soc.* **1983**, *105*, 1679. (b) Doherty, N. M.; Fildes, M. J.; Forrow, N. J.; Knox, S. A. R.; Macpherson, K. A.; Orpen, A. G. *J. Chem. Soc., Chem. Commun.* **1986**, 1355. See also the following review: (c) Geoffroy, G. L.; Bassner, S. *Adv. Organomet. Chem.* **1988**, *28*, 1.

(13) Photochemistry of the diiron μ-methylene complex $Cp^*_2Fe_2(\mu\text{-}CH_2)(\mu\text{-}CO)(CO)_2$ at low temperatures was reported recently: Spooner, Y. H.; Mitchell, E. M.; Bursten, B. E. *Organometallics* **1995**, *14*, 5251.

(14) Casey, C. P.; Austin, E. A. *J. Am. Chem. Soc.* **1988**, *110*, 7106.

(15) Although catalytic formation of H_2 and $Me_3SiSiMe_3$ was observed during conversion of **4** to **5a** and **6a**, the turnover numbers were at most 2−3 (rt −50 °C).

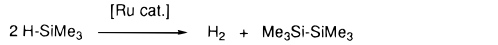

Table 1. NMR and IR Data for Silylated and Stannylated μ-Methylene Complexes[a]

			^{1}H-NMR				^{13}C-NMR				IR
complex	solv	temp	CH_2	Cp	H	Si(Sn)R_3	CH_2	Cp	CO	Si(Sn)R_3	ν(C≡O)
5a	CD_2Cl_2	rt	6.87 (d, 3.6), 6.93 (d, 3.6)	5.21	−10.01	0.37	110.0 (t, 144)	88.6 (d, 177), 90.1 (d, 178)	203.3, 205.7	6.9 (q, 119)	1924
		−60	6.80 (d, 3.6), 6.90 (d, 3.6)	5.21, 5.26	−10.09	0.37					
5b	C_6D_6	rt	6.97 (d, 3.6), 7.07 (d, 3.6)	4.98	−9.95	0.33−1.28 (m, Et)	109.0 (t, 143)	88.5 (d, 179), 89.4 (d, 179)	203.3, 205.3	9.7 (q, 119), 10.9 (t, 118)	1924
5d	CD_2Cl_2	rt	6.95 (d, 2.9), 7.11 (d, 2.9)	5.07	−10.08	0.59, 0.70, 7.26−7.68 (m, Ph)	110.7 (t, 142)	88.5 (d, 178), 90.1 (d, 178)	203.5,. 205.4	*b*	1926
		−20	6.93 (d, 2.9), 7.07 (d, 2.9)	5.04, 5.13	−10.09	0.58, 0.70, 7.31−7.64 (m, Ph)					
5e	CD_2Cl_2	−10	*c*	4.72, 5.06	−10.19	7.1−7.6 (m, Ph)	113.2 (t, 144)	88.7 (d, 180), 90.2 (d, 178)	204.3, 205.3	*d*	1930
5f	CD_2Cl_2	−20	6.87 (d, 2.9), 4.58 (d, 2.9)	5.26, 5.31	−9.98	3.53	105.3 (t, 147)	89.1 (d, 175)	201.8, 205.0	51.0 (q, 142)	1936
6a	$CDCl_3$	rt	6.13	5.14		0.32	117.0 (t, 141)	90.6 (d, 178)	206.7	3.9 (q, 118)	1904
6b	$CDCl_3$	rt	6.30	5.20		0.7−1.1 (m, Et)	116.8 (t, 141)	89.9 (d, 178)	206.5	9.9 (q, 145), 11.9 (t, 120)	1905
6c	$CDCl_3$	rt	6.21	5.12		0.55−1.42 (m, Pr)	118.5 (t, 138)	89.6 (d, 178)	206.2	18.7 (q, 140), 19.6 (t, 125), 24.0 (t, 114)	1906
6d	$CDCl_3$	rt	6.41	4.78		0.57, 0.64, 7.27−7.64 (m, Ph)	120.8 (t, 141)	90.9 (d, 177)	207.2	5.1 (q, 120), 5.9 (q, 119)	1908
6e	$CDCl_3$	rt	7.15	4.53		7.2−7.6 (m, Ph)	128.3 (t, 143)	91.8 (d, 180)	207.8	*f*	1915
6f	$CDCl_3$	rt	7.06	5.31		3.59	108.4 (t, 144)	90.7 (d, 179)	205.5	51.1 (q, 142)	1924
11	$CDCl_3$	rt	6.55[g] (d, 13),[c] 9.00, 9.31	4.47,[g] 4.67, 4.83, 5.12		*h*	109.6[g] (ddd, 7, 135, 144), 110.6 (ddd, 9, 137, 142)	87.8 (d, 174),[g] 88.3 (d, 174), 89.3 (d, 174), 90.9 (d, 173)	201.0,[g] 201.6	*i*	1915, 1750
cis-**12a**	$CDCl_3$	rt	10.10 [j]	5.21		0.15	131.3 [j] (d, 112)	89.3 (d, 178)	199.2, 247.2	2.9 (q, 117)	1973, 1937, 1782
trans-**12a**	$CDCl_3$	rt	9.15 [j]	5.28, 5.36		0.23	*k*				
cis-**12b**	$CDCl_3$	rt	10.32 [j]	5.12		7.05−7.84	115.4[g,j] (d, 116)	90.0 (d, 178)[g]	197.8[g]	*l*	1984[g]
trans-**12b**	$CDCl_3$	rt	9.15 [j]	4.98, 4.99		7.05−7.84	117.5 [j] (d, 112)	90.9 (d, 178), 91.6 (d, 178)	200.0, 240.0, 244.2		1942, 1788
13a	$CDCl_3$	rt	7.95[j] (d, J_{PH} 13)	4.44, 4.87		0.33, 7.34−7.55 (Ph)	125.6[j] (d, 120)	89.7 (d, 176), 89.9 (d, 182)	201.6, 254.0 (d, J_{PH} = 11)	*m*	1917, 1747
13b[g]	$CDCl_3$	rt	8.15[j,g] (d, J_{PH} 13)[c]	4.24,[g] 4.78, 4.45, 4.82		7.19−7.78	112.8[g,j] (dd, 117, J_{PC} 4)[o]	87.5 (d, 176),[g] 89.1 (d, 176), 89.9 (d, 178), 90.6 (d, 178)	200.7,[g] 202.7, 235.2, 250.6 (d, J_{PC} 11)	*n*	1917,[g] 1747
20a	C_6D_6	rt	6.59 (d, 2.9), 6.90 (d, 2.9)	4.71, 4.89	−10.68	0.39	101.0 (t, 142)	87.8 (d, 178), 88.6 (d, 178)	202.4, 205.5	−5.4 (q, 127)	1918
20b	C_6D_6	rt	6.09 (d, 2.9), 6.54 (d, 2.9)	4.30, 4.39	−10.12	*p*	99.7 (t, 142)	87.4 (d, 178), 88.6 (d, 177)	205.5	*q*	1915
20c	C_6D_6	rt	*c*	4.05, 4.30	−10.22	6.46−7.39 (m, Ph)	102.1 (t, 145)	87.7 (d, 178), 88.9 (d, 179)	203.2, 205.3	*r*	1925
21a	$CDCl_3$	rt	5.59	5.07		0.24	98.7 (t, 139)	86.8 (d, 178)	204.4	−5.8 (q, 127)	1899
21b	$CDCl_3$	rt	5.68	5.13		*s*	95.5 (t, 139)	87.1 (d, 178)	205.2	*t*	1895

[a] Chemical shifts are reported in ppm downfield from TMS. Multiplicity and coupling constants (in Hz; J_{HH} or J_{CH} unless otherwise stated) are shown in parentheses. The signals without the sign of multiplicity are singlets. IR spectra were recorded in CH_2Cl_2. [b] δ_C (Ph) 127.2 (d, 155), 127.9 (d, 160), 133.3 (d, 151), 147.7 (s). [c] Overlapped with the Ph signal. [d] δ_C 126−137 (d), 140.6 (s), 142.1 (s), 145.0 (s). [e] δ_C 127.1 (d, 155), 127.9 (d, 160), 133.8 (d, 157), 146.9 (s). [f] δ_C 127.1 (d, 156), 128.1 (d, 158), 136.3 (d, 156), 141.7 (s), 142.3 (s), 143.5 (s). [g] A mixture of *cis*- and *trans*-isomers. [h] δ_H 7.24−7.65 (m; Ph and one of the CH_2 signals). [i] δ_C 127.6, 127.8 (d, 161, para), 129.49, 129.54 (dd, 3 (J_{CP}), 161, meta), 134.2, 134.3 (dd, 10 (J_{CP}), 157), 135.6, 136.3 (d, 32 (J_{CP}), ipso). [j] μ-*CH*SiR$_3$ signal. [k] Minor component. [l] δ_C(Ph) 127.5, 128.9, 136.8, 139.1; 127.2, 128.7, 136.5, 138.8. [m] δ_C(PPh_3) 136.4 (d, J_{PC} = 41, ipso), 134.4 (dd, J_{PC} = 9, J_{CH} = 161), 129.6 (d, J_{CH} = 161), 127.7 (dd, J_{CP} = 9, J_{CH} = 163). [n] δ_C(Ph) 127−142. [o] One of the signals could not be located. [p] δ_H 0.90 (t, J = 6 Hz, CH_3), 0.97 (t, J = 8 Hz, $SnCH_2$), 1.53−1.71 ($(CH_2)_2$). [q] δ_C 14.0 (q, 123, CH_3), 14.1 (t, 126, $SnCH_2$), 28.1, 30.5 (t × 2, J = 122, $(CH_2)_2$). [r] δ_C(Ph) 128.1 (d, 159), 128.4 (d, 159), 137.2 (d, 154), 144.1 (s). [s] 0.90 (t, J = 6, CH_3), 0.97 (t, J = 8, $SnCH_2$), 1.53−1.71 [$Sn(CH_2CH_2CH_2CH_3)$]. [t] δ_C 13.7 (q, 124, CH_3), 14.0 (t, $^1J_{C-H}$ = 125 Hz, $^1J_{C-Sn}$ = 165 Hz, $SnCH_2$), 27.6, 30.2 (t × 2, 124, $(CH_2)_2$).

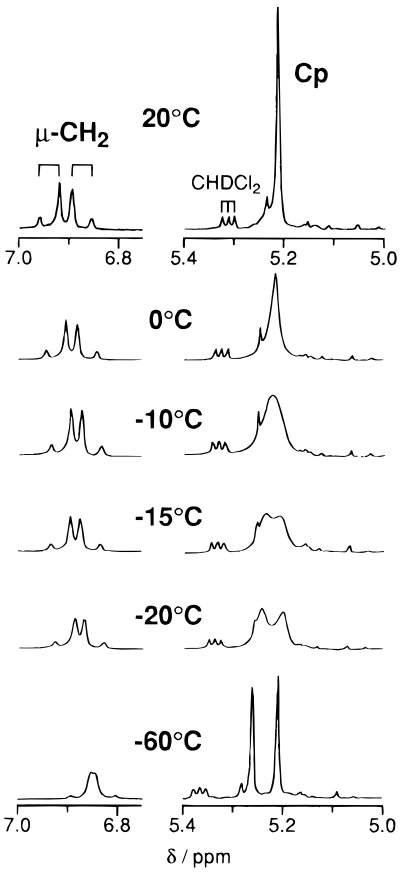

Figure 1. Variable-temperature ^{1}H-NMR spectra of **5a** (μ-CH_2 and Cp regions) observed in CD_2Cl_2 at 90 MHz.

Upon warming of the sample, a ^{1}H-NMR spectrum consistent with an apparent C_s-symmetrical structure was obtained. The Cp resonances (^{1}H-NMR) broadened and coalesced above 0 °C without any notable change of the AB quartet pattern of the μ-CH_2 signals. (The ^{13}C-NMR Cp signals of **5** appeared as two sharp signals at room temperature.) As for the mechanism, an intermolecular one can be excluded, since external $DSiMe_3$ is not incorporated into **5a** on the time scale of the VT measurement and **5a** is stable under reduced pressure. Therefore the fluxional behavior of **5** should be explained in terms of an intramolecular mechanism involving concerted migration of the hydride and SiR_3 groups between the two Ru centers. Plausible mechanisms for the metal-promoted dyotopic rearrangement of the *cis*- and *trans*-isomers[16] are shown in Scheme 6, where the only difference is the change of the configuration at the Ru centers. In the case of the *cis*-isomer,

Scheme 6

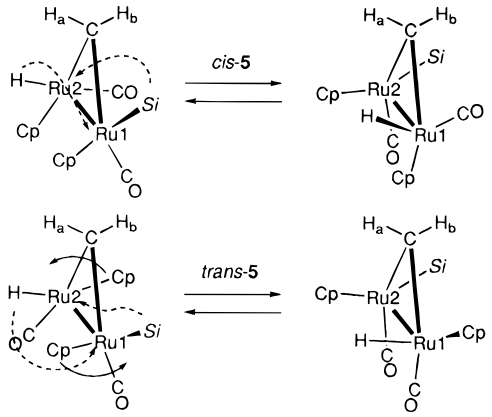

(i) the two mobile groups migrate on the side closer to the μ-CH_2 ligand and (ii) the configuration at Ru (with respect to the Cp, CO, CH_2, and Ru moieties) and the overall geometry of the $Cp_2Ru_2(\mu\text{-}CH_2)(CO)_2$ part are retained throughout the process. On the other hand, the Ru atoms in the *trans*-isomer are attacked by the mobile groups from the back-side of the leaving groups and inversion of the Ru centers should result. In both mechanisms the inequivalent two methylene protons appear as an AB quartet, when the migration occurs at a rate faster than the NMR line-broadening time scale. A third mechanism involves conversion to an η^2-H−Si coordinated structure (like **7** in Scheme 5), where intramolecular exchange with CO attached to the adjacent Ru atom and subsequent Si−H oxidative addition regenerates **5′**. Because the first mechanism can accomplish the migration via least motion of the Ru auxiliaries, it may be preferable to the others. Therefore the configuration of **5** is tentatively assigned to the *cis*-structure.[16] Similar rapid intramolecular migration of a silyl group on a dinuclear system was reported for the diruthenium μ-methylene complex (η^5-C_5Me_5)$Ru_2(\mu\text{-}CH_2)(\mu\text{-}Cl)(SiMe_3)$ by Girolami et al.[17]

The C_2-symmetrical structure of the disilyl complex **6** (*trans*-configuration) has been readily characterized on the basis of the equivalent Cp, CH_2, CO, and SiR_3 signals and the absence of a μ-CO ligand. Furthermore the structure of the $SiMe_2Ph$ (**6d**) and $SiPh_3$ derivatives (**6e**·hexane) has been determined by X-ray crystallography. An overview of **6d** and top and side views of its core part are shown in Figure 2, and ORTEP views of **6e** are included in the Supporting Information, because the core structure is quite similar to that of **6d** as compared in Table 2. The Ru−Ru distances are longer than that of **1**[5f] by ca. 0.1 Å probably owing to the disappearance of the bridging carbonyl ligand, although significant difference is not observed for other parameters such as the Ru−CH_2 and Ru−CO lengths.

The intramolecular migration of the SiR_3 groups as observed for **5** (Scheme 6) does not operate for the disilyl complex **6**, because the diastereotopic Me_2 groups in **6d** are inequivalent even at 110 °C in toluene-d_8.

(ii) Intra- and Intermolecular Exchange Processes of the Hydrido−Silyl−μ-Methylene Complexes 5. In addition to the intramolecular migration process mentioned above (Scheme 6), complexes **5** show quite complicated exchange behavior as summarized in

(16) *cis* and *trans* refer to the configuration of the two Cp (or CO) ligands with respect to the dimetallacyclopropane core [(μ-CH_2)Ru_2]. When it is assumed that H and SiR_3 groups project to the same side as does the μ-CH_2 ligand (as observed for **6**), two isomers are possible for each of the two configurations and Scheme 6 shows only one structure for each. When configuration at the Ru atoms in the partial structure $Cp_2Ru_2(\mu\text{-}CH_2)(CO)_2$ [**5** − (H + SiR_3)] is considered, the configuration is retained in the case of the *cis*-structure [R(Ru1)−*S*(Ru2) ↔ *R*(Ru1)−*S*(Ru2)] but it is inverted in the case of the *trans*-structure [*R*(Ru1)−*R*(Ru2) ↔ *S*(Ru1)−*S*(Ru2)]. It is difficult to assign the structure by the spectral data alone, although one of reviewers suggests a *trans*-structure on the basis of the similar δ_H values of H_a and H_b (cf. **1**). In addition, several mechanisms such as the third mechanism and *cis*−*trans* isomerization are possible for the present fluxional behavior. A reviewer suggests the third mechanism because of the lack of the fluxional behavior of the disilyl complex **6**, for which the η^2-structure like **7** is not possible. But, in this case, too, a definite conclusion cannot be obtained on the basis of the results obtained so far.

(17) Lin, W.; Wilson, S. R.; Girolami, G. S. *Organometallics* **1994**, *13*, 2309.

Table 2. Selected Structural Parameters for the μ-Methylene Complexes 6d,e and 21a[a]

	6d	6e·hexane	21a	*cis*-1[b]
		Bond Lengths		
Ru1−Ru2	2.8054(6)	2.8298(9)	2.796(2)	2.707(1)
Ru1−Si1(Sn1)	2.417(2)	2.429(2)	2.649(1)	
Ru1−C1	2.074(6)	2.053(8)	2.06(1)	2.077(6)
Ru1−C11−15	2.211−2.232(7)	2.230−2.292(7)	2.22−2.27(2)	2.219−2.276(9)
Ru1−C16	1.831(6)	1.826(8)	1.62(2)	1.852(6)
Ru2−Si2(Sn2)	2.422(2)	2.429(2)	2.649(2)	
Ru2−C1	2.076(6)	2.047(8)	2.09(1)	2.079(5)
Ru2−C21−25	2.231−2.308(8)	2.225−2.324(8)	2.22−2.30(2)	2.231−2.290(8)
Ru2−C26	1.843(7)	1.822(8)	1.87(2)	1.844(7)
C1−H1A	1.09(5)	0.85(5)		
C1−H1B	0.96(5)	0.93(5)		
		Bond Angles		
Ru1−C1−Ru2	85.1(2)	87.3(3)	83.8(4)	81.3(2)
Ru2−Ru1−Si1(Sn1)	109.51(4)	108.75(5)	118.27(5)	
Ru2−Ru1−C1	47.5(2)	46.3(2)	48.2(3)	49.3(2)
Ru2−Ru1−C16	79.5(2)	82.7(2)	88.0(6)	98.7(2)
Si1(Sn1)−Ru1−C1	78.2(2)	75.5(2)	74.2(3)	
Si1(Sn1)−Ru1−C16	81.0(2)	82.6(2)	80.4(6)	
C1−Ru1−C16	109.0(3)	109.4(3)	99.1(7)	89.1(3)
Ru1−Ru2−Si2(Sn2)	108.91(5)	109.29(5)	117.28(5)	
Ru1−Ru2−C1	47.4(2)	46.4(2)	48.0(3)	49.4(2)
Ru1−Ru2−C26	80.8(2)	80.0(2)	90.2(5)	96.5(2)
Si2(Sn2)−Ru2−C1	77.0(2)	74.9(2)	73.2(3)	
Si2(Sn2)−Ru2−C26	81.4(2)	83.6(3)	76.7(5)	
C1−Ru2−C26	120.9(3)	106.3(3)	98.2(6)	85.0(2)

[a] Bond lengths in Å and bond angles in deg. [b] Reference 5f.

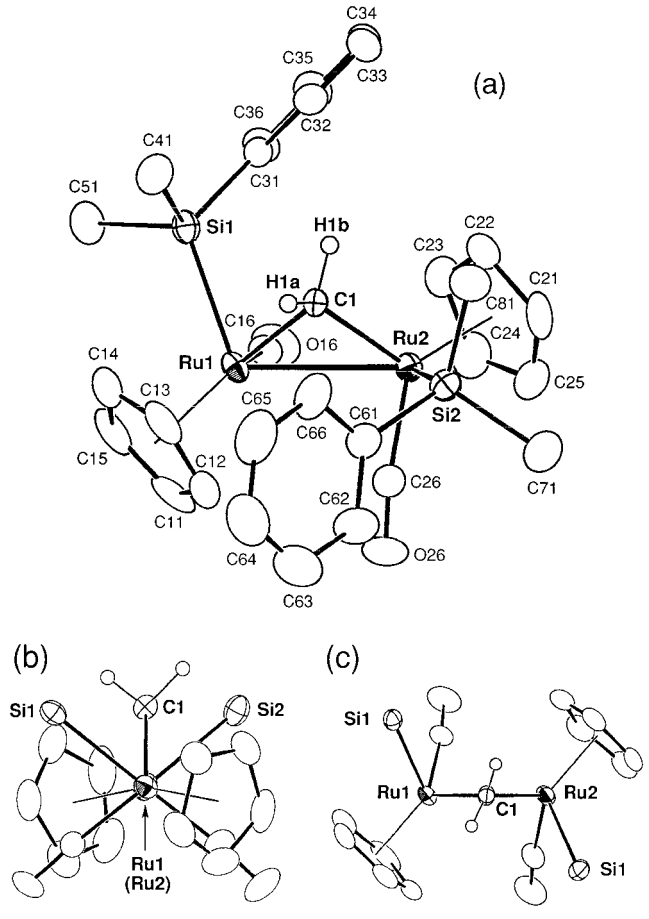

Figure 2. Molecular structure of **6d** drawn at the 30% probability level: (a) an overview; (b) a top view; (c) a side view.

Scheme 7. Process a is an intramolecular H exchange between the hydride and CH_2 atoms, and by way of processes b and c both of the H and SiR_3 groups of external hydrosilane are incorporated into **5**.

Scheme 7

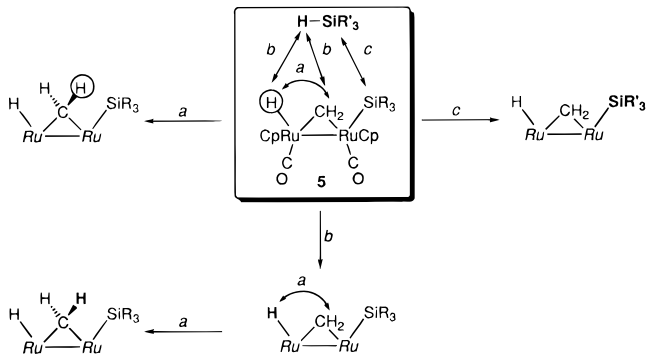

Treatment of **4** with $DSiMe_3$ resulted in complete H−D scrambling of the hydride and μ-methylene parts (eq 3). The result may be explained by either of the

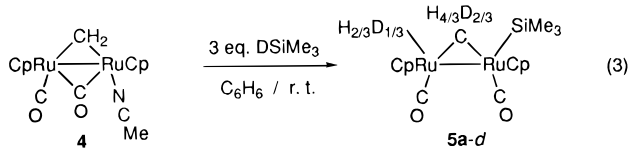

mechanisms involving equilibrium with a coordinatively unsaturated methyl intermediate **9** or **10** via reversible reductive elimination−oxidative addition of a C−H(D) bond (Scheme 8).[18] Path a is initiated by formation of the deuteride complex **5**-d_1 followed by H−D scrambling via the methyl intermediate **9**-d_1. In the second mechanism (path b) H−D exchange takes place at the stage of the initial adduct **8**-d_1 by way of another methyl intermediate **10**-d_1. Differentiation of these two mechanisms was attempted by a low-temperature NMR experiment. When a CD_2Cl_2 solution of **4** and $DSiMe_2Ph$ was warmed from −60 °C, gradual formation of **5d**-*d* was observed above −30 °C as shown in Figure 3. In

(18) Another possible mechanism for conversion of **8** into **5** involves R_3Si-group migration instead of the H migration shown in Scheme 8.

Scheme 8

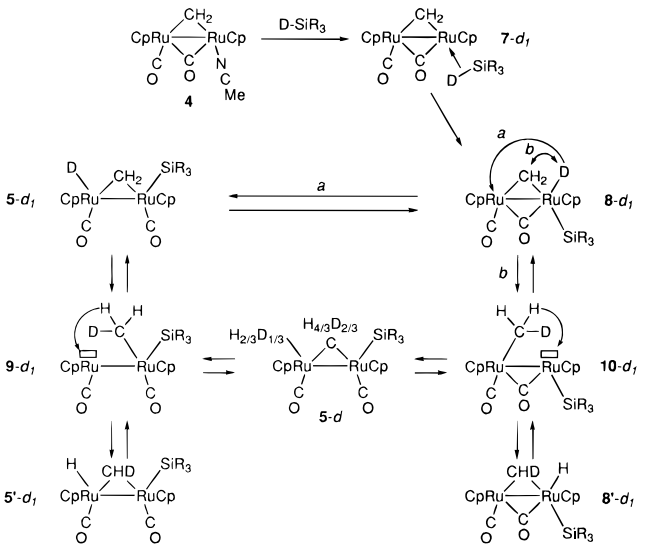

Figure 4 distribution of H atoms in the μ-CH_2 and hydride parts is plotted against the measurement temperature, and it is found that the μ-CH_2 + CHD/hydride intensity ratio of **5d**-*d* is constant (ca. 1.5) throughout the temperature range. Although we expected detection of the deuteride complex **5c**-d_1(a) (see the structure shown in Figure 3) with the ratio of 2/0, a mixture of all the possible three isomers **5c**-d_1(a−c) was present even at a very early stage of the reaction. This result indicates that the H−D exchange follows the second mechanism (path b) or the H−D exchange in path a (**5**-d_1 → **9**-d_1 → **5′**-d_1) is much faster than the preceding intramolecular hydride transfer (**8**-d_1 → **5c**-d_1). On the basis of the reaction with $HSnPh_3$ (see below) supporting the viability of **9**, path a is preferable to path b, though the mechanisms cannot be differentiated by the data obtained so far. Bergman et al. reported a similar intramolecular hydrogen shift on early−late heterobimetallic (ELHB) hydrido−μ-methylene complexes, $Cp_2Ta(\mu\text{-}CH_2)_2Ir(\eta^5\text{-}C_5Me_5)(H)$(*Ta*−*Ir*) and $Cp_2Ta(\mu\text{-}CH_2)_2M(H)_2(CO)(L)$(*Ta*−*M*) (M = Rh, Ir; L = CO,PPh_3).[19] In the case of the former complex, isomerization needs heating at 105 °C probably because of the robust Ir−H bond.

In addition to the above-mentioned intramolecular process, intermolecular exchange processes are observed for **5**. Treatment of **5a** with 5 equiv of $DSiMe_3$ for 5 h at rt produced the deuterated product **5a**-d_3 along with **6a**-d_2 and $HSiMe_3$ (eq 4). Furthermore addition of an

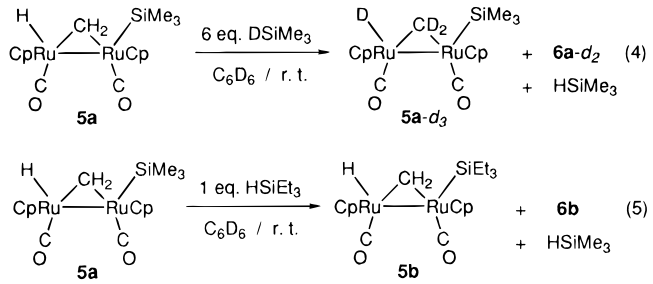

equimolar amount of $HSiEt_3$ to **5a** afforded **5b** (rt, 1 h; 60% conversion, 80% selectivity; eq 5) along with a small amount of **6b**. Thus not only the hydride and C*H*$_2$ atoms but also the SiR_3 group in **5** exchange with external hydrosilane.

(19) (a) Hostetler, M. J.; Butts, M. D.; Bergman, R. G. *J. Am. Chem. Soc.* **1993**, *115*, 2743. (b) Butts, M. D.; Bergman, R. G. *Organometallics* **1994**, *13*, 2668.

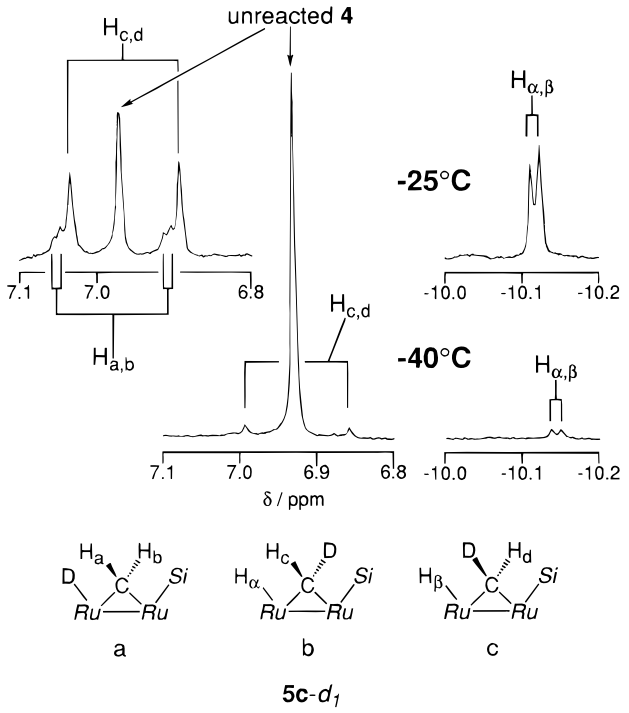

Figure 3. ^{1}H-NMR spectra (μ-CH_2 and hydride regions) of a low-temperature reaction between **4** and $DSiMe_2Ph$ in CD_2Cl_2 observed at 400 MHz.

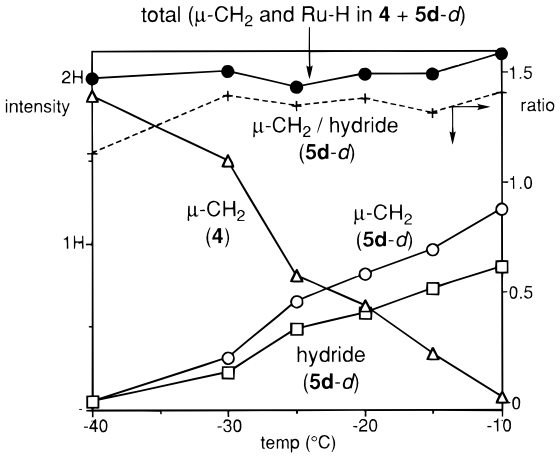

Figure 4. Distribution of H atoms during the reaction between **4** and $DSiMe_2Ph$ in CD_2Cl_2.

(iii) Intermolecular Exchange Processes of the Disilyl Complexes 6. Treatment of **6b** with 6 equiv of $DSiMe_3$ for 1 h at ambient temperature produced **6a**-d_2 (eq 6). Furthermore heating a sealed benzene-d_6 solution of a mixture of **6a** and $HSiPh_3$ (3 eq) for 2 h at 60 °C resulted in quantitative formation of **6e** accompanied by elimination of $HSiMe_3$ (eq 7), though no apparent reaction was observed at room temperature. When the resulting sealed tube was left for 24 h at ambient temperature, the $SiMe_3$ complex **6a** was recovered quantitatively. Thus the CH_2 and SiR_3 moieties in **6** also exchange with external $HSiR'_3$, and judging from eq 7, **6** bearing a less bulky R group is more stable than that with a bulky group.

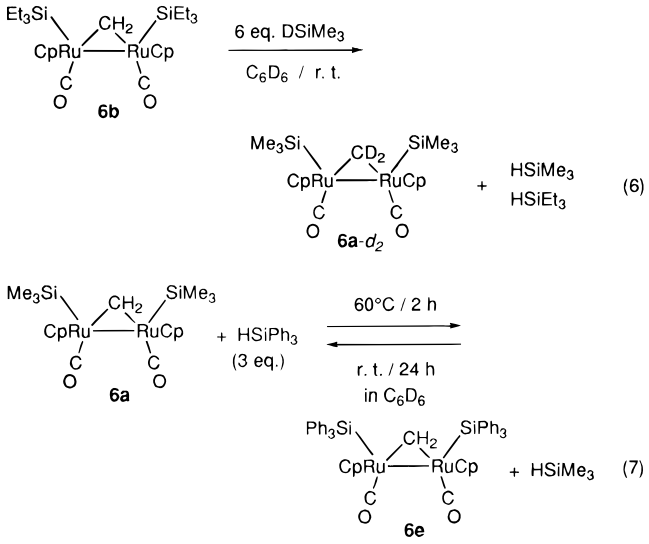

Mechanism of Intermolecular Exchange Processes of the Silyl-μ-Methylene Complexes 5 and 6. In order to find a clue to the mechanism of the incorporation of hydrosilane into the diruthenium μ-methylene complexes **5** and **6** (Scheme 4), participation of coordinatively unsaturated intermediates was examined at first by treatment of the two silylated μ-methylene complexes **5** and **6** with trapping agents (L: 2e-donor).

Addition of CO or PPh_3 (L) to the hydrido−silyl species **5a** resulted in spontaneous, quantitative formation of adducts $Cp_2Ru_2(\mu\text{-}CH_2)(\mu\text{-}CO)(CO)L$ [**1** (L = CO), **11** (L = PPh_3)] accompanied by elimination of $HSiMe_3$ (eq 8). This result can be interpreted by taking into

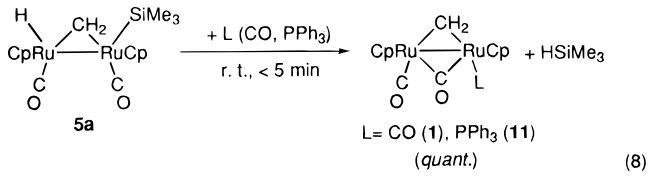

account the equilibrium between **5** and **7** (Scheme 9; see also Schemes 5 and 8). Replacement of the weakly coordinating η^2-H−SiR_3 ligand in **7** would give **1** and **11**. The intermolecular exchange reaction of the H and R_3Si groups in **5** (eqs. 4 and 5) can also be accounted for in terms of the η^2-H−SiR_3 intermediate **7**. Exchange with external $HSiR'_3$ would result in the formation of the scrambled products. Therefore both of the H- and R'_3Si parts should be incorporated into **5** by way of a single reaction (paths b and c in Scheme 7).

The disilyl complexes **6a,e** did not react with CO and PPh_3 at ambient temperature. However, heating their benzene solution at 80 °C resulted in quantitative formation of isomeric mixtures of μ-silylmethylene complexes, *cis*- and *trans*-$Cp_2Ru_2(\mu\text{-}CHSiR_3)(\mu\text{-}CO)(CO)(L)$ [**12** (L = CO), **13** (L = PPh_3)], also accompanied by elimination of hydrosilane (1 equiv) as observed by ^{1}H-NMR (eq 9). Though several isomers are possible for **12** (2 *cis* + 1 *trans*) and **13** (2 *cis* + 2 *trans*), a lesser number of isomers are detected by NMR (**12a**, 1 *cis* + 1 *trans*; **12b**, 2 isomers; **13a**, 1 isomer; **13b**, 2 isomers). The $SiMe_3$ derivatives **12a** and **13a** have been structurally characterized by X-ray crystallography (Figures 5 and 6 and Table 3), and the structure is in accord with the change in the coupling pattern of the bridging

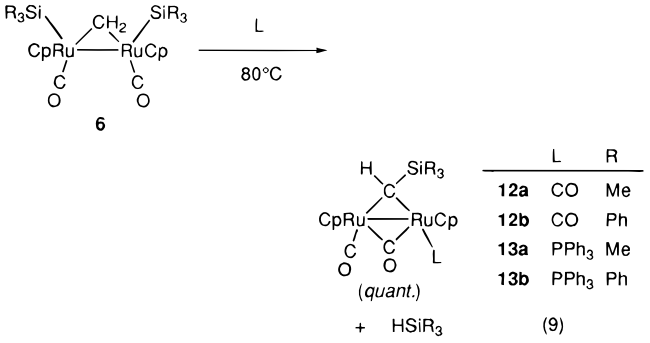

	L	R
12a	CO	Me
12b	CO	Ph
13a	PPh_3	Me
13b	PPh_3	Ph

carbon signal [triplet (μ-CH_2 in **6**) → doublet (μ-$CHSiR_3$ in **12** and **13**)] and appearance of a ν(μ-CO) vibration. The most striking structural feature of **12** and **13** is that the SiR_3 group initially bonded to the Ru center is transferred to the bridging methylene carbon atom. In addition, one of the two silyl groups is eliminated from the organometallic products as is consistent with the results of GLC and NMR analyses. The core parts of **12a** and **13a** resemble that of *cis*-**1** as compared in Table 3.

A plausible formation mechanism of **12** and **13** prompted by this structural change is delineated in Scheme 9 involving activation of C−H, Si−H, and Si−C bonds. Thermolysis of **6** may induce reductive elimination of the methylene carbon atom and one of the two silyl groups to give a coordinatively unsaturated silylmethyl species **14**. Subsequent oxidative addition of a C(α)−H bond in the resultant CH_2SiR_3 group gives rise to the μ-silylmethylene intermediate **15**, which is finally converted to **12** and **13** via replacement of the η^2-coordinated silane ligand (**16**) by a trapping agent (L). This mechanism has been confirmed by observation of the reverse process. When the η^2-intermediate **16** (R = Me) is generated by treatment of the MeCN-stabilized, labile μ-silylmethylene species **17** with $HSiMe_3$ (eq 10), the instantaneous reaction results in quantita-

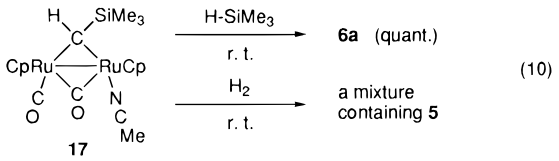

tive formation of **6a**, which follows Si−H oxidative addition, C−H reductive elimination, and finally Si−C(sp^3) oxidative addition (Scheme 9). Recombination of the CH_2 and silyl groups closely related to the present system was also reported by Girolami et al. for the diruthenium silyl−μ-methylene complex (η^5-C_5Me_5)Ru_2(μ-CH_2)(μ-Cl)($SiMe_3$)[17] mentioned above. For example, protonation with CF_3COOH at 25 °C afforded $Cp^*_2Ru_2(\mu\text{-}CHSiMe_3)(\mu\text{-}Cl)(\mu\text{-}CF_3COO)$ with a Si−C bond accompanied by evolution of H_2. Although Scheme 9 suggests that thermolysis of **6** in the absence of a trapping agent may afford the hydrido−silyl−μ-silylmethylene species $Cp_2Ru_2(\mu\text{-}CHSiR_3)(H)(SiR_3)(CO)_2$, a complicated reaction mixture is merely obtained.

A similar reaction sequence can be depicted for the η^2-H_2 intermediate **18** as also shown in Scheme 9. The reaction pathway may lead to the formation of the hydrido−silyl−μ-methylene species **5** via reductive elimination of the H and μ-$CHSiR_3$ moieties followed by oxidative addition of the CH_2−SiR_3 bond (**19**). In contrast to the reaction of **17** with hydrosilanes, the

Scheme 9

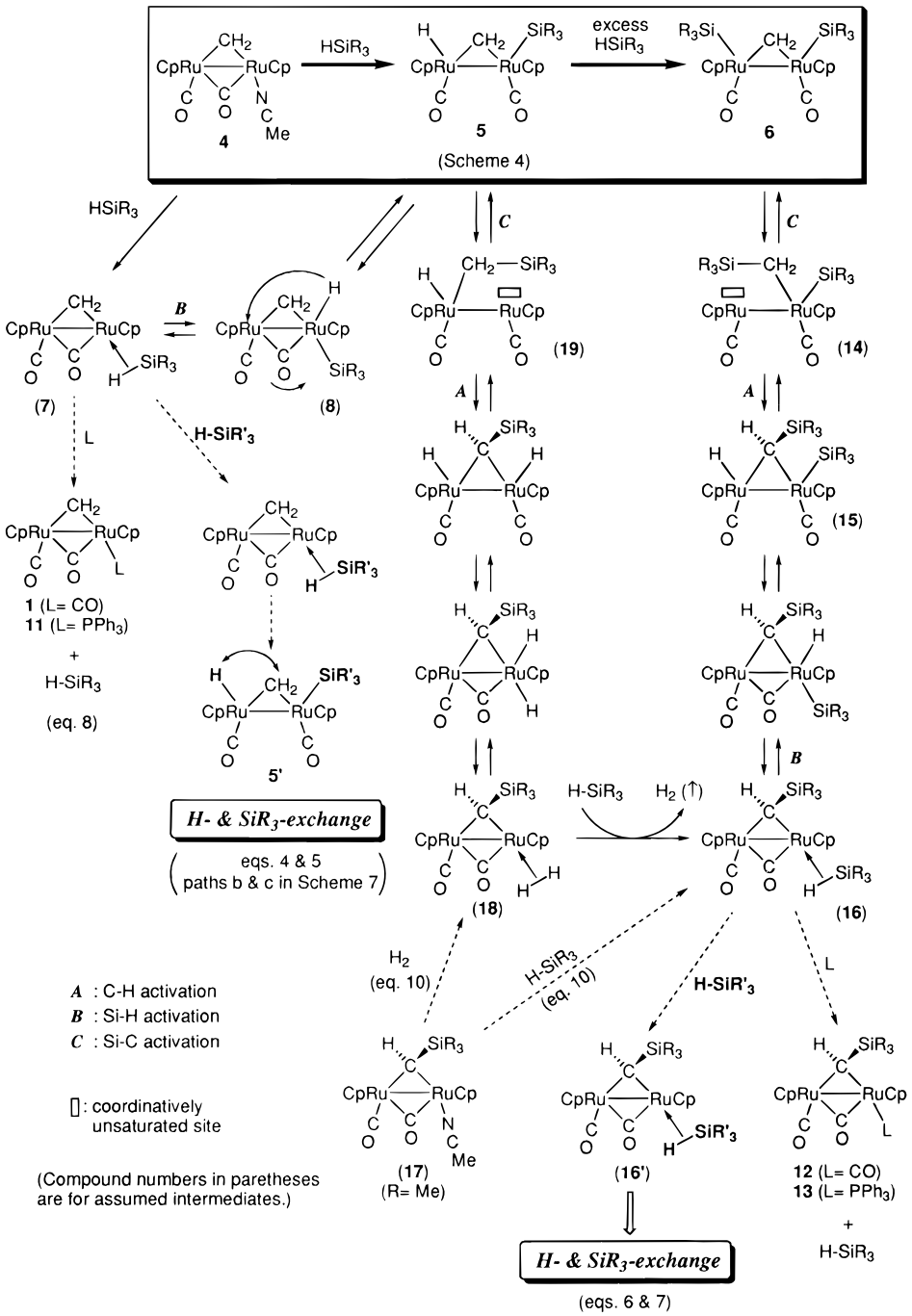

reaction with H_2 afforded a mixture containing a small amount of **5a** (eq 10). This is probably due to the higher reactivity of the resulting **5** toward H_2 compared to that of the starting compound **17** (see below). Anyway it has proved that the reactions of **17** with hydrogen and hydrosilane are quite similar to each other. Furthermore, if the η^2-H_2 ligand in **18** is replaced by H−SiR_3 (**18** → **16**), the reaction sequence summarized in Scheme 9 can account for the mechanism of the conversion of **5** into **6** (Scheme 4). Thus the two silylated μ-methylene complexes **5** and **6** are linked with each other by a combination of oxidative addition−reductive elimination processes of Si−H, Si−C, and C−H bonds. The conversion should be driven forward by diffusion of H_2 into the gas phase.

The mechanism can also explain the intermolecular exchange of the μ-CH_2 and SiR_3 groups in **6** (eqs 6 and 7), which would be caused by substitution of the η^2-coordinated silane in **16** by external silane ($HSiR'_3$).

It has proved that the hydrido−silyl−μ-methylene intermediate **5** is in equilibrium with the isomeric form (**5**″), the coordinatively unsaturated methyl (**9**) and silylmethyl intermediates (**19**), and the η^2-H−SiR_3 species (**7**) by way of intramolecular H and R_3Si migration and reversible oxidative addition−reductive elimination processes of C−H, Si−H, and Si−C(sp^3) bonds (Scheme 10). Although Si−C(sp^2) bond cleavage is often observed as typically exemplified by redistribution of arylhydrosilanes in the presence of a transition metal species,[20] examples of Si−C(sp^3) bond cleavage processes are still quite rare. They may be classified into (i) intermolecu-

(20) See, for example: Bell, L. G.; Gustavson, W. A.; Thanedar, S.; Curtis, M. D. *Organometallics* **1983**, *2*, 740.

Table 3. Selected Structural Parameters for the μ-Methylene Complexes 12a and 13a[a]

12a		13a		*cis*-**1**[b]
		Bond Lengths		
Ru1−Ru1*	2.698(1)	Ru1−Ru2	2.7349(8)	2.707(1)
Ru1−C1	2.092(5)	Ru1−C1	2.122(6)	2.077(6)
		Ru2−C1	2.109(6)	2.079(5)
Ru1−C17	1.838(5)	Ru1−C16	1.829(7)	1.852(6)
Ru1−C16	2.046(6)	Ru1−C26	2.073(6)	2.019(4)
		Ru2−C26	1.984(7)	2.035(6)
C1−Si1	1.841(7)	C1−Si1	1.857(7)	
Si1−C31	1.863(9)	Si1−C31	1.867(8)	
Si1−C32	1.866(7)	Si1−C32	1.881(8)	
		Si1−C33	1.870(8)	
Ru1−C(11−15)	2.207−2.298(6)	Ru1−C(11−15)	2.239−2.325(7)	2.219−2.276(9)
		Ru2−C(21−25)	2.219−2.291(7)	2.231−2.290(8)
C16−O16	1.154(8)	C26−O26	1.171(7)	1.156(8)
C17−O17	1.140(6)	C16−O16	1.158(8)	1.179(6)
		Ru2−P1	2.294(2)	
C1−H1	0.91(6)	C1−H1	0.90(6)	1.02, 0.84(7)
		Bond Angles		
Ru1−C1−Ru1*	80.3(2)	Ru1−C1−Ru2	80.5(2)	81.3(2)
Ru1−C1−Si1	128.8(2)	Ru1−C1−Si1	119.4(3)	
		Ru2−C1−Si1	128.3(3)	
Ru1*−Ru1−C1	49.8(1)	Ru2−Ru1−C1	49.5(2)	49.3(2)
Ru1*−Ru1−C16	48.7(1)	Ru2−Ru1−C26	46.2(2)	48.4(2)
Ru1*−Ru1−C17	101.3(2)	Ru2−Ru1−C16	86.3(2)	
		Ru1−Ru2−C1	49.9(2)	49.4(2)
		Ru1−Ru2−C26	49.0(2)	

[a] Bond lengths in Å and bond angles in deg. [b] Reference 5f.

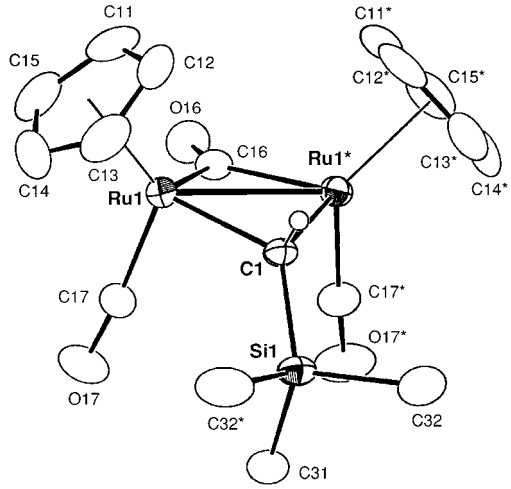

Figure 5. Molecular structure of **12a** drawn at the 30% probability level.

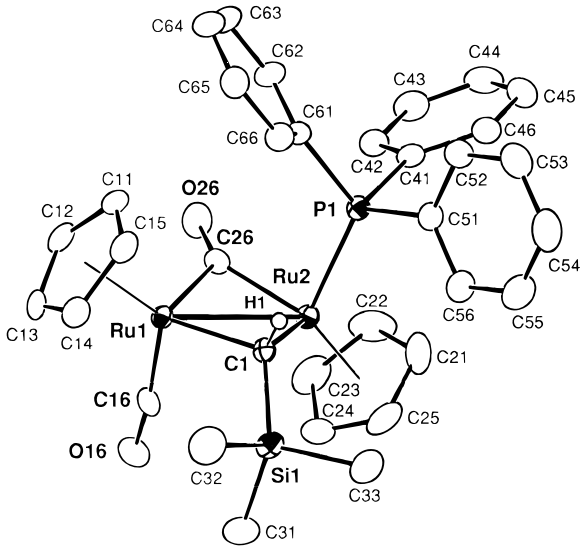

Figure 6. Molecular structure of **13a** drawn at the 30% probability level.

lar reaction of simple silanes and strained cyclosilanes and (ii) intramolecular version on alkylsilyl and silylalkyl complexes $M-(CH_2)_n-SiR_3$ ($n = 0-2$) giving an alkyl−silene species ($n = 0$), an alkylidene−silyl species ($n = 1$), or a silyl−ethylene species ($n = 2$).[21] The present system (**5** → **19** and **14** → **6** in Scheme 9) falls in the second category.

Reaction of $Cp_2Ru_2(\mu\text{-}CH_2)(\mu\text{-}CO)(CO)(MeCN)$ (4) with Hydrostannanes Leading to Stannylated μ-Methylene Species $Cp_2Ru_2(\mu\text{-}CH_2)(X)(SnR_3)(CO)$ [20 (X = H) and 21 (X = SnR_3)]. Reactivity of the MeCN complex **4** toward hydrostannanes ($HSnR_3$) has been studied as a comparative system of the $HSiR_3$ reduction discussed above. As a result, it is found that $HSnR_3$ shows reactivities quite similar to that of hydrosilanes (Scheme 11). Quantitative formation of the hydrido−stannyl−μ-methylene intermediate **20** is followed by gradual conversion to the distannyl−μ-methylene complex **21** with the exception of the case of $HSnPh_3$ (see below). The structure of the $(SnMe_3)_2$ derivative (**21a**) with virtual C_2 symmetry determined by X-ray crystallography (Figure 7 and Table 2) is similar to that of the Si analogues **6b**,**e**.

The spectroscopic features of the stannyl complexes **20** and **21** (Table 1) are essentially the same as those of the silyl complexes **5** and **6**, respectively, except for the absence of fluxional property via intramolecular H and R_3Sn group exchange (interconversion between **20** and **20′**; cf. Scheme 4), which may come from the robust Ru−Sn bond compared to the Ru−Si bond. In accord with this observation, reaction rates of exchange of H

(21) See, for example: (a) Yamashita, H.; Tanaka, M.; Honda, K. *J. Am. Chem. Soc.* **1995**, *117*, 8873. A few examples of catalytic redistribution of functionalized alkylsilanes (e.g. halosilanes) are also known. (b) Curtis, M. D.; Epstein, P. S. *Adv. Organomet. Chem.* **1981**, *19*, 213. For intramolecular reactions, see ref 17. A reaction system closely related to ours was reported in this paper. See also references cited in these papers.

Scheme 10

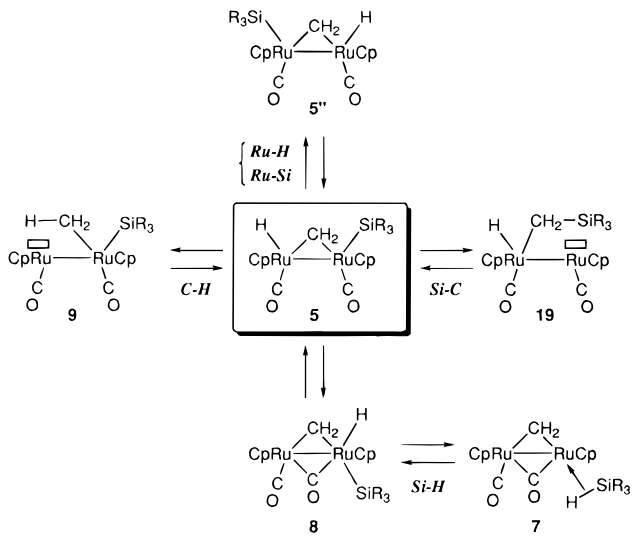

Scheme 11

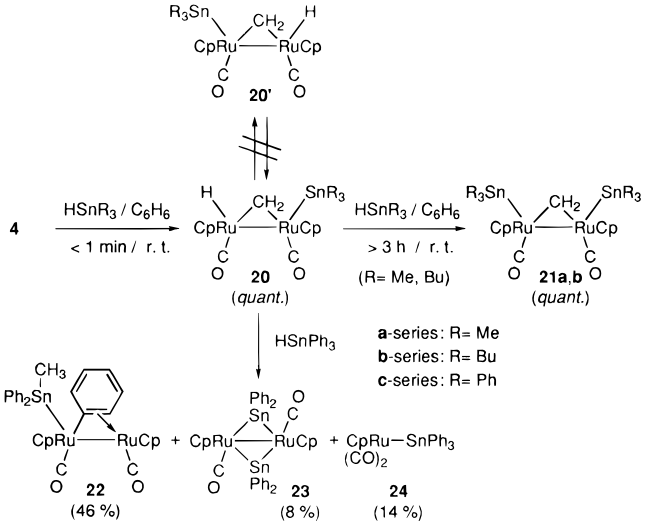

and SnR_3 groups in **20** with external $HSnR_3$ (Scheme 12) and formation of the distannyl complexes (**20** → **21**; Scheme 11) were slower than those of the corresponding Si systems, and treatment of **20a** with CO and PPh_3 did not result in elimination of $HSnMe_3$ (cf. eq 8).[22] However, exchange between the hydride and CH_2 atoms in **20** proceeded as fast as that of the Si system (reaction a in Scheme 7), since ^{1}H-NMR spectra of a low-temperature reaction mixture of **4**-d_2 and $HSnMe_3$ revealed formation of almost equal amounts of all the three possible isotopomers **20a**-d_2(a−c) even at an early stage of the reaction (Figure 8[23] and Scheme 12). Further standing at ambient temperature caused exchange with external $HSnMe_3$ in a manner similar to the Si system (eq 8) as indicated by the appearance of a pair of doublets (^{1}H-NMR) assignable to **4**-d_1(f) or **4**-d_0.

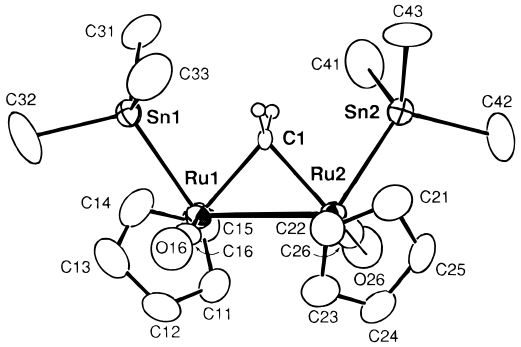

Figure 7. Molecular structure of **21a** drawn at the 30% probability level.

Scheme 12

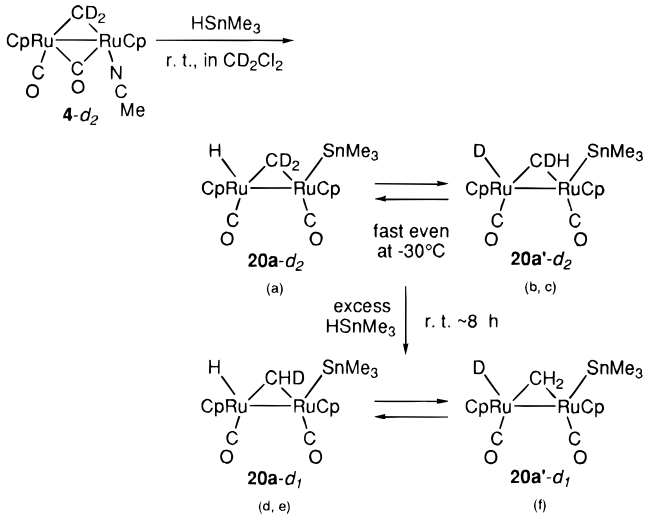

Reaction of **4** with triphenylhydrostannane ($HSnPh_3$) produced **20c** at first (Scheme 11), but upon standing at rt, it was not converted to **21c** but to a mixture containing the bridging phenyl complex **22**, the bridging stannylene complex **23**,[24] and the mononuclear stannyl complex $CpRu(CO)_2SnPh_3$ (**24**).[25] The structure of the μ-phenyl complex **22** has been confirmed by X-ray crystallography (Figure 9 and Table 4). Characteristic structural features are (i) the μ-η^1:η^2 coordination of the bridging phenyl group arising from cleavage of one of the Sn−Ph bonds and (ii) transformation of the μ-CH_2 ligand into the $SnCH_3$ functional group. A cyclohexatrienyl-like structure (C31−C36) is suggested by the localized double-bond character as indicated by bond lengths summarized in Chart 1, though bond alteration is not so clear. The trend in the changes in the C−C bond lengths of the phenyl groups is similar to the previously reported heterotrinuclear μ-η^1:η^2-phenyl cluster compound (Chart 1).[26] μ-η^1:η^2-Aryl complexes, in particular, C_6H_5 complexes, are a rather rare class of compounds, though more examples are reported for μ-η^1:η^1-derivatives[26,27] and μ-η^1:η^2-heteroaryl complexes (e.g.

(22) Thermolysis of **21a** in the presence of a 2e-donor did not afford the μ-stannylmethylene complex analogous to **12** (**13**) but a μ-stannylene complex $Cp_2Ru_2(\mu\text{-}CH_2)(\mu\text{-}SnMe_2)(CO)_2$ with quantitative elimination of $SnMe_4$: Hua, R.; Akita, M.; Moro-oka, Y. Unpublished result.

(23) From the spectra shown in Figure 8 it is impossible to discriminate the isomers **20a**-d_2(b,c) from **20a**-d_1(d,e), respectively, as indicated by a reviewer. However, because the intensity ratios of the μ-CH_2 and Ru−H signals at lower temperatures (~1:1) are in accord with **20a**-d_2(b,c) and the appearance of a pair of doublets ($H_{e,f}$) after 8 h at rt suggests the formation of **20a**-d_1, the low-temperature products have been assigned to **20a**-d_2(b,c) and the $H_{a,b,c,d}$ signals come come from the structures shown in Figure 8.

(24) The structure of **23** was confirmed by X-ray crystallography, though it could not be refined owing to the poor quality of the crystal.

(25) Ellis, J. E.; Faltynek, R. A.; Hentges, S. G. *J. Organomet. Chem.* **1975**, *120*, 389.

(26) (a) Farrugia, L. J.; Miles, A. D.; Stone, F. G. A. *J. Chem. Soc., Dalton Trans.* **1984**, 2415. (b) Dickson, R. S.; Jenkins, S. M.; Skelton, B. W.; White, A. H. *Polyhedron* **1988**, *7*, 859.

(27) Cluster compounds containing a μ-η^1:η^2-phenyl ring which is linked to another metal center at the m- or p-positions are known. See, for example: Chi, Y.; Shu, H.-Y.; Peng, S.-M.; Lee, G.-H. *J. Chem. Soc., Chem. Commun.* **1991**, 1023.

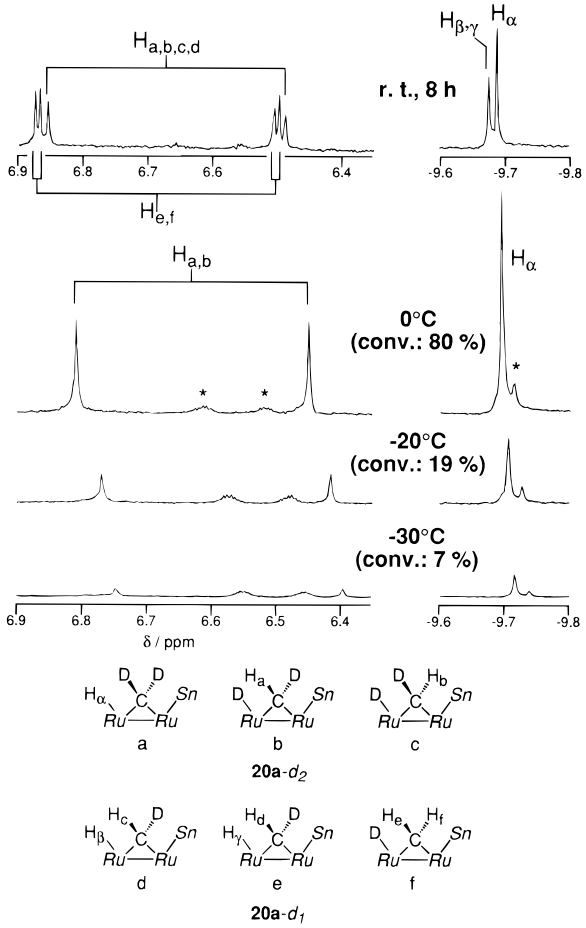

Figure 8. ^{1}H-NMR spectra (μ-CH_2 and hydride regions) of a low-temperature reaction between **4**-d_2 and $HSnMe_3$ in CD_2Cl_2 observed at 400 MHz. (Peaks with asterisks are due to impurities.)

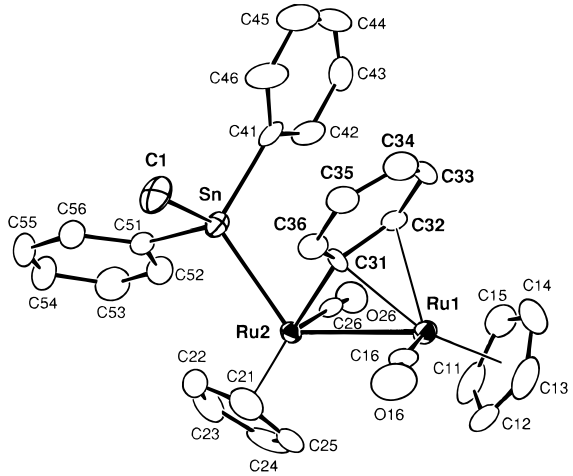

Figure 9. Molecular structure of **22** drawn at the 30% probability level.

furyl and thienyl complexes).[28] Partial loss of aromaticity is also demonstrated by NMR data assigned with the aid of H−H COSY and C−H HETCOR spectra. The C32−H32 signals are observed in considerably higher field [δ_H 5.08 (d, J = 6.1 Hz); δ_C 77.7 (d, J = 150 Hz)], whereas the C31 signal (δ_C 162.8) is shifted to lower field. These NMR features are similar to those of μ-η^1:

(28) (a) Himmelreich, D.; Müller, G. *Chem. Ber.* **1985**, *297*, 341. (b) Arce, A. J.; Manzur, J.; Marquez, M.; De Sanctis, Y. *J. Organomet. Chem.* **1991**, *412*, 177.

Table 4. Selected Structural Parameters for 22[a]

Bond Lengths			
Sn−Ru2	2.636(2)	Ru2−C26	1.81(2)
Sn−C1	2.14(2)	O16−C16	1.15(2)
Sn−C41	2.18(2)	O26−C26	1.17(2)
Sn−C51	2.14(1)	C−C (C11−15)	1.35−1.42(3)
Ru1−C11−15	2.13−2.25(2)	C−C (C21−25)	1.35−1.41(2)
Ru1−C16	1.85(2)	C−C (C41−46)	1.32−1.41(2)
Ru2−C21−25	2.23−2.26(2)	C−C (C51−56)	1.36−1.42(2)

Bond Angles			
Ru2−Sn−C1	114.8(5)	Ru1−C31−Ru2	79.9(4)
Ru2−Sn−C41	115.9(3)	Ru1−C31−C32	74.1(8)
Ru2−Sn−C51	110.3(4)	Ru1−C31−C36	119(1)
C1−Sn−C41	105.7(6)	Ru2−C31−C32	124(1)
C1−Sn−C51	102.7(6)	Ru2−C31−C36	121(1)
C41−Sn−C51	106.3(5)	C32−C31−C36	115(1)
Ru2−Ru1−C16	95.8(5)	Ru1−C32−C31	69.6(7)
Ru2−Ru1−C31	47.5(3)	Ru1−C32−C33	119.2(9)
Ru2−Ru1−C32	74.6(3)	C31−C32−C33	121(1)
Sn−Ru2−Ru1	125.36(5)	C32−C33−C34	119(2)
Sn−Ru2−C26	84.0(4)	C33−C34−C35	121(2)
Sn−Ru2−C31	76.9(4)	C34−C35−C36	121(2)
Ru1−Ru2−C26	82.9(4)	C31−C36−C35	122(2)
Ru1−Ru2−C31	52.5(4)	C−C−C(C41−46)	117−125(2)
Ru1−C16−O16	172(2)	C−C−C(C51−56)	119−124(2)
Ru2−C26−O26	171(1)		

[a] Bond lengths in Å and bond angles in deg. See also Chart 1.

Chart 1

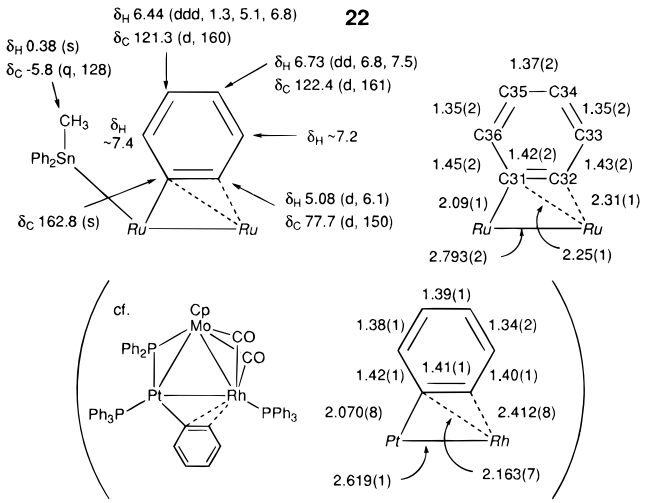

η^2-alkenyl complexes.[29] Because **22** is not fluxional at rt, the η^2-coordination has proved to be rigid.

The formation of **22** should be initiated by C−H reductive elimination from **20c** leading to the unsaturated methyl intermediate **25** (Scheme 13). The Sn−Ph part is so nucleophilic that subsequent irreversible migration of a Ph group gives the μ-stannylene intermediate **26**. Subsequent reductive elimination of the CH_3 and $SnPh_2$ parts followed by η^2-coordination of the Ph group furnishes **22**. The isolation of **22** containing the CH_3 group supports the viability of the methyl species **9** assumed as an intermediate for the H−D exchange (Scheme 8). The formation mechanism of **23** has remained unknown, though elimination of methane (~30%) and benzene (~120%) was detected by GLC analysis of a reaction mixture.

Consideration of the Formation Mechanism of Methane from 1. (i) Reaction of the Silylated μ-Methylene Complexes 5 and 6 with Hydrogen.

(29) See for example, ref 5a.

The hitherto described results reveal that the most stable species present in a reaction mixture of **4** and hydrosilane is the disilyl−μ-methylene complex **6**. It is notable that catalytic evolution of 2−3 equiv of H_2 was observed during the reaction.[15] Therefore it is anticipated that methane formation (eq 1) may follow hydrogenolysis of **6**. As expected, treatment of **6** with H_2 produced methane along with a complicated organometallic mixture containing the trinuclear hydride complex, $Cp_3Ru_3(\mu\text{-}H)_3(\mu\text{-}CO)_3$[30] as a major component (eq 11). But remarkable difference in the reaction rates

6 $\xrightarrow{H_2\ (1\ atm)}$ CH_4 + $CH_3\text{-}CH_3$ + $CH_3\text{-}CH_2\text{-}CH_3$ + $Cp_3Ru_3(\mu\text{-}H)_3(\mu\text{-}CO)_3$ (**31**) (11)

R= Me (**6a**) [a]	18 (96)	0	0	trace (22)
R= Et (**6b**)	53	46	0	85
R= n-Pr (**6c**)	102	0	38	45

[a] Yields in parentheses are for the reaction at 65°C for 7 h. Other reactions were carried out for 3 days at r. t.

was observed for the $SiMe_3$ (**6a**) and $SiEt_3$ derivatives (**6b**). The reaction of the $SiEt_3$ derivative (**6b**) proceeded even at room temperature, whereas the $SiMe_3$ derivative **6a** produced methane when heated above 50 °C. Let us point out that ethane was formed from **6b**. In order to confirm the source of ethane (coupling of μ-methylene ligands or decomposition of the $SiEt_3$ group), hydrogenolysis of the n-propyl derivative **6c** was carried out. The reaction of **6c** proceeded at room temperature in a manner similar to **6b** to give a mixture of methane and propane. Because no trace of ethane was detected in the reaction mixture, ethane and propane arose from decomposition of the SiR_3 part in **6b**,**c**, respectively, probably via oxidative addition of the Si−R bond. Then the carbon and hydrogen source of methane arising from H_2 treatment of **6a** was determined by labeling experiments. As a result, the ^{13}C content of methane arising from a ^{13}C-labeled sample $Cp_2Ru_2(\mu\text{-}{*}CH_2)(SiMe_3)_2$ $({*}CO)_2$ (**6a**-^{13}C) (*C: ca. 25% ^{13}C-enriched) was found to be close to that of the starting compound **6a**-^{13}C (eq 12), and D_2

6a-^{13}C $\xrightarrow[65°C,\ 7\ h]{H_2}$ $^{*}CH_4$ (12)

6a-d_2 $\xrightarrow[65°C,\ 7\ h]{D_2}$ CD_4 (13)

treatment of $Cp_2Ru_2(\mu\text{-}CD_2)(SiMe_3)_2(CO)_2$ (**6a**-d_2) afforded CD_4 (eq 13), though H−D exchange was evident. It was concluded that H_2 treatment of **6a** produced methane via hydrogenolysis of the μ-CH_2 moiety.

Hydrogenolysis of the hydrido−silyl−μ-methylene intermediate **5** proceeded much faster than the disilyl complex **6**. The reaction was completed within 12 h to produce methane along with a complicated mixture of organometallic products (eq 14).

5a $\xrightarrow[r.\ t.,\ <12\ h]{H_2}$ CH_4 (72 %) (14)

(30) Forrow, N. J.; Knox, S. A. R.; Morris, M. J.; Orpen, A. G. *J. Chem. Soc., Chem. Commun.* **1983**, 234.

Scheme 13

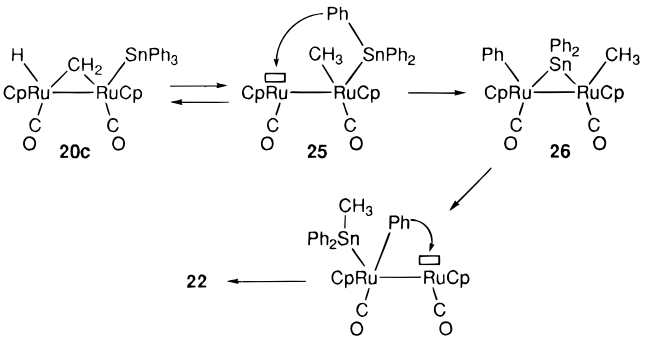

Scheme 14

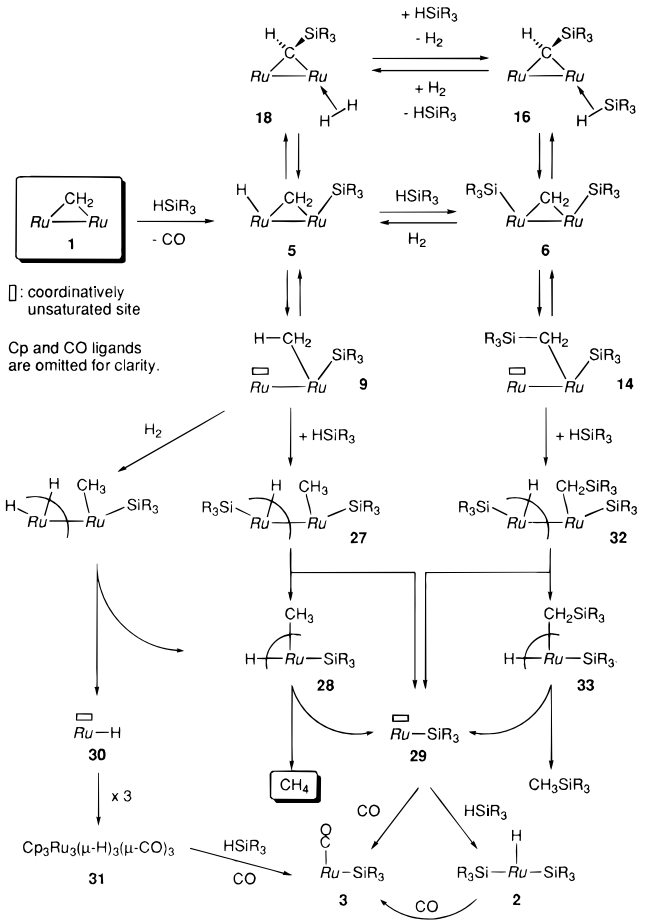

(ii) Methane Formation Mechanism from 1 and $HSiR_3$. On the basis of the reaction sequence summarized in Scheme 9 and the hydrogenolysis experiments discussed above, we propose a plausible formation mechanism of methane from the μ-methylene complex **1** as shown in Scheme 14. Decarbonylation followed by oxidative addition of $HSiR_3$ affords the hydrido−silyl−μ-methylene intermediate **5**, and further reaction with excess $HSiR_3$ leads, via η^2-bonded intermediates **18** and **16**, to the formation of the disilyl−μ-methylene complex **6**, which is the major organometallic species present in a reaction mixture. But **6** may not be the direct precursor for production of methane. The hydrido−silyl species **5** is converted to the disilyl complex **6** with evolution of H_2 as discussed above. In the sealed tube reaction the evolved H_2 is still present in the gas phase. In addition, catalytic formation of 2−3 equiv of H_2 was noted.[15] Therefore the formation of **6** may be reverted by the action of H_2 under the reaction

Scheme 15

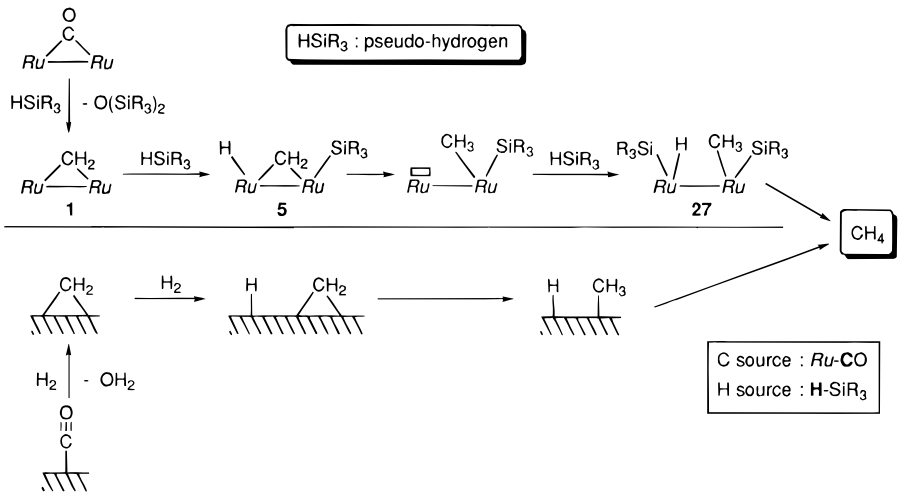

conditions to regenerate **5**, which is in equilibrium with the coordinatively unsaturated methyl species **9**, as confirmed by the labeling experiments. Subsequent reductive elimination followed by oxidative addition of $HSiR_3$ may give the dinuclear hydrido−methyl intermediate **27**. Further reductive elimination of the H and $CpRu(CO)(CH_3)(SiR_3)$ parts generates the mononuclear hydrido−methyl species **28**, final reductive elimination from which produces methane.

Reductive elimination at the last stage of the reaction releases 2 equiv of coordinatively unsaturated silyl species **29**, which will be trapped by either $HSiR_3$ or CO (released at the initial stage) to afford the mononuclear organometallic products **2** or **3**, respectively. Another route to methane involves hydrogenolysis of **9** releasing **28** and a mononuclear hydride species **30**. Trimerization of **30** produces the trinuclear hydride complex $Cp_3Ru_3(\mu\text{-}H)_3(\mu\text{-}CO)_3$ (**31**).[5e] Further reaction of the hydride cluster **31** with $HSiR_3$ affords the mononuclear hydride complex **3** as confirmed by a separate experiment. Similar reaction sequence starting from the disilyl complex **6** would afford the methylsilane (**6** → **14** → **32** → **33** → CH_3SiR_3).

Concluding Remarks. Reduction of the diruthenium μ-methylene complex **1** with $HSiR_3$ produces methane via silylated μ-methylene species **5** and **6**. The μ-methylene complex **1** itself can be obtained by deoxygenative reduction of the ruthenium carbonyl complex $Cp_2Ru_2(\mu\text{-}CO)_2(CO)_2$ with H_2SiR_2 (path b in Scheme 2) as we reported previously.[6f] Thus combination of these two reaction systems leads to successful modeling of the thorough reaction sequence of methanation via Fischer−Tropsch mechanism (Scheme 15). The features of the present system are as follows: (i) Every transformation takes place on the dinuclear system. (ii) A CO ligand in $Cp_2Ru_2(CO)_4$ is converted into the μ-CH_2 species (**1**) by the action of the pseudo-hydrogen, i.e. $HSiR_3$ (deoxygenative reduction). (iii) The resultant μ-methylene species (**1**) is further reduced by $HSiR_3$ to produce CH_4 via the hydrido−μ-methylene species **5** and hydrido−methyl intermediates such as **27** and **28**. (iv) CH_2−H coupling on **5** leads to equilibrium with the methyl intermediate **9**. (v) The carbon and hydrogen atoms in methane come from CO attached to Ru and *H*SiR_3 employed as a H_2 equivalent, respectively. These aspects have been realized by the reaction features of hydrosilane as a pseudo-hydrogen as mentioned in the Introduction.

Detailed analysis of dynamic behavior and H−D exchange processes of the silylated μ-methylene species **5** and **6** reveal that Si−H, C−H, and Si−C bonds are cleaved quite readily on a dinuclear reaction field. This means that, if a bond is disposed with appropriate orientation toward a reactive metal center, it may be cleaved efficiently via oxidative addition. In the present case, the orientation of the ligand to be cleaved is regulated through the σ-bond to one metal center and bond activation occurs on the other unsaturated metal center (e.g. **9**, **14**, **19**). This type of bond activation belongs to "bimetallic activation", a concept proposed by Suzuki.[31]

Finally, further systematic study on the reactivity peculiar to a dinuclear system, typically displayed by the present study, would lead to exploitation of new methods for functionalization of organosilanes.[32]

Experimental Section

General Methods. All manipulations were carried out under an inert atmosphere by using standard Schlenk tube techniques. Ether, hexanes, and toluene (Na−K alloy) and CH_2Cl_2 and CH_3CN (P_2O_5) were treated with appropriate drying agents, distilled, and stored under argon. Dinuclear μ-methylene complexes **1**[33] and **4**[5j] were prepared according to the literature procedures. Hydrosilanes and $HSnMe_3$ were prepared by reduction of corresponding chlorosilane and $BrSnMe_3$ (prepared by exothermic conproportionation of $SnMe_4$ and $SnBr_4$) with $LiAlH_4$, respectively. Labeling experiments were carried out as described for the H compounds by using appropriate labeled compounds. The μ-CD_2 complex **1**-d_2 was prepared by treatment of $Cp_2Ru_2(CO)_4$[34] with $LiDBEt_3$.[33] The ^{13}CO-labeled μ-methylene complex **1**-^{13}C (μ-CH_2 and CO carbon atoms ca. 25% ^{13}C-enriched) was prepared by treatment of $Cp_2Ru_2(CO)_4$-^{13}C with $LiHBEt_3$.[33] [$Cp_2Ru_2(CO)_4$-^{13}C was obtained by carbonylation [^{13}CO (1−2 atm); >90% ^{13}C-enriched] of $Cp_2Ru_2(CO)_3(MeCN)$[5c,6j] in benzene at room temperature.] Deuteriosilanes were prepared by treatment of appropriate chlorosilanes with $LiAlD_4$. Chromatography was performed

(31) Takao, T.; Yoshida, S.; Suzuki, H.; Tanaka, M. *Organometallics* **1995**, *14*, 3856 and references cited therein.
(32) Recent progress in activation of organosilicon compounds on metal complexes is reviewed in the following paper: Braunstein, P.; Knorr, M. *J. Organomet. Chem.* **1995**, *500*, 21.
(33) Berry, D. H.; Bercaw, J. E. *Polyhedron* **1988**, *7*, 759.
(34) Doherty, N. M.; Knox, S. A. R.; Morris, M. J. *Inorg. Synth.* **1990**, *28*, 189.

on alumina [column, aluminum oxide, activity II−IV (Merck Art. 1097); preparative TLC, aluminum oxide $60PF_{254}$ (Type E) (Merck Art. 1103)]. ^{1}H- and ^{13}C-NMR spectra were recorded on JEOL EX-90 (^{1}H, 90 MHz), GX-270 (^{1}H, 270 MHz; ^{13}C, 67 MHz), EX-400 (^{1}H, 400 MHz; ^{13}C, 100 MHz), and GX-500 spectrometers (^{1}H, 500 MHz; ^{13}C, 125 MHz). Solvents for NMR measurements containing 1% TMS were dried over molecular sieves, degassed, distilled under reduced pressure, and stored under Ar. IR and MS spectra were obtained on a JASCO FT/IR 5300 spectrometer and a Hitachi M-80 mass spectrometer, respectively. Volatile products were quantified by GLC [hydrocarbons (Porapak Q/FID); H_2, CO (Molecular Sieves 5A/TCD); Hitachi gas chromatograph 163].

Thermolysis of the μ-Alkylidene Complexes in the Presence of Hydrosilane. To a C_6D_6 solution (0.4 mL) of **1** (15.8 mg, 0.029 mmol) in an NMR tube was added $HSiMe_3$ (20 μL, 0.17 mmol). The NMR tube was sealed by a torch and heated at 170 °C in a GLC oven. The reaction was monitored occasionally by ^{1}H-NMR. When **1** was consumed, the yields of organometallic products **2** and **3** were determined by ^{1}H-NMR (internal standard: residual C_6D_5H). Then the NMR tube was placed in a glass autoclave filled with Ar together with a magnetic stirring bar. After the autoclave was closed, it was shaken vigorously so that the NMR tube was broken. After addition of propane and butane (internal standards) through a rubber septum, the yields of CH_4 and $SiMe_4$ were determined by GLC analysis of the gas and liquid phases. The organometallic products were identified after separation with preparative TLC. **2** (colorless oil): ^{1}H-NMR (C_6D_6) 4.56 (5H, s, Cp), 0.51 (18H, s, $(SiMe_3)_2$), −10.87 (s, 1H, Ru−H). ^{13}C-NMR (C_6D_6) 201.9 (s, CO), 88.1 (d, J = 177 Hz, Cp), 10.3 (q, J = 119 Hz, $SiMe_3$). IR (CH_2Cl_2) ν(C≡O) 1942 cm^{-1}. Anal. Calcd for $C_{12}H_{24}OSi_2Ru$: C, 42.20; H, 7.08. Found: C, 42.48; H, 7.28. **3** was identified by comparison with the reported data.[5]

Formation of Hydrido−Silyl−μ-Methylene Species 5. To a benzene suspension of **4** was added $HSiR_3$ (1.2 equiv) via a microsyringe. As soon as $HSiR_3$ was added, the solid **4** dissolved to give a deep orange red homogeneous solution. Soon after that all the volatiles were removed under reduced pressure to leave orange red oily product **5**. Quantitative formation of **5** was observed by ^{1}H-NMR experiments carried out in C_6D_6. Attempted isolation of a pure sample of **5** was unsuccessful because of its thermal lability. Then **5** was characterized on the basis of the spectroscopic data (Table 1) and comparison with the unequivocally characterized disilyl complexes **6** (see text).

The reaction with $DSiMe_3$ was carried out in a similar manner.

Preparation of Disilyl-μ-Methylene Complexes 6. To a benzene suspension (5 mL) of **4** (60.0 mg, 0.13 mmol) was added $HSiR_3$ (0.32 mmol) via a syringe. The resulting homogeneous solution was left overnight at ambient temperature or heated for 15 min above 50 °C. Volatiles were removed under reduced pressure, and the residue was subjected to preparative TLC separation (eluent: CH_2Cl_2/hexanes = 1/5−1/8). Complex **6a** was isolated by recrystallization from MeOH, and complexes **6b**−**f** were isolated by recrystallization from CH_2Cl_2−hexanes mixed solvent. All the **6**-type compounds were isolated as orange yellow solid. The spectroscopic data are summarized in Table 1. Isolated yields and analytical data of **6** are summarized as follows (analytically pure samples of **6a**,**b**,**f** were not obtained due to the high solubility in organic solvents). **6a** (35% yield): Calcd for $C_{19}H_{30}O_2Si_2Ru_2$: C, 41.60; H, 5.47. Found: C, 41.07; H, 5.36. **6b** (27% yield): Calcd for $C_{25}H_{42}O_2Si_2Ru_2$: C, 47.46; H, 6.64. Found: C, 45.97; H, 7.01. **6c** (53% yield): Calcd for $C_{31}H_{54}O_2Si_2Ru_2$: C, 51.95; H, 7.54. Found: C, 51.91; H, 7.37. **6d** (33% yield): Calcd for $C_{29}H_{34}O_2Si_2Ru_2$: C, 51.78; H, 5.06. Found: C, 51.32; H, 5.21. **6e** (46% yield): Calcd for $C_{49}H_{42}O_2Si_2Ru_2$: C, 63.89; H, 4.60. Found: C, 63.44; H, 4.98. **6f** (70% yield): Calcd for $C_{19}H_{30}O_8Si_2Ru_2$: C, 35.38; H, 4.65. Found: C, 34.56; H, 4.61.

Exchange Reactions of 5 and 6. A crude sample of **5** generated as described above or an isolated sample of **6** (5−10 mg) was taken in an NMR tube. After addition of C_6D_6 (0.5 mL) a ^{1}H-NMR spectrum was recorded to check the initial concentration of **5** or **6** by comparison with the intensity of the residual C_6D_5H signal. Then appropriate hydrosilane or deuteriosilane was added and capped with a rubber septum (or sealed by a torch when the sample was heated). The extent of the D incorporation and conversion was monitored occasionally by ^{1}H-NMR.

Low-Temperature Reaction of 5a with $DSiMe_2Ph$ (Figures 3 and 4). An NMR tube containing a CD_2Cl_2 solution (0.5 mL) of **4** (5.3 mg, 0.012 mmol) was capped with a rubber sepum. To the sample cooled at −78 °C was added $DSiMe_2Ph$ (3 μL, 0.018 mmol) via a microsyringe through the rubber septum. After being shaken vigorously, the sample tube was transferred to the NMR probe precooled at −60 °C. The probe temperature was raised to the temperature indicated in Figure 4, and ^{1}H-NMR spectra were recorded: δ_H (at −40 °C) 6.86, 6.99 (s, $H_{c,d}$), 6.92 (s, μ-CH_2 of **4**), −10.14, −10.15 (s, $H_{\alpha,\beta}$); δ_H (at −25 °C) 6.91, 7.05 (d, J = 4 Hz, $H_{a,b}$), 6.89, 7.03 (s, $H_{c,d}$), (s, μ-CH_2 of **4**), −10.12, −10.13 (s, $H_{\alpha,\beta}$).

Reaction of 5a with CO or PPh_3. CO was passed through a C_6D_6 solution of **5a** in situ prepared as described above, or PPh_3 (1.2 equiv) was added to a C_6D_6 solution of **5a**. ^{1}H-NMR analysis after 10 min revealed quantitative formation of **1** or **11**, respectively. **11** was isolated as yellow crystals after preparative TLC separation followed by crystallization from CH_2Cl_2−hexanes. Anal. Calcd for $C_{31}H_{27}O_2PRu_2$: C, 56.02; H, 4.09. Found: C, 56.32; H, 4.30.

Thermolysis of 6a,e in the Presence of CO. A benzene solution (2 mL) of **6a** (16.3 mg, 0.03 mmol) was placed in a 10 mL-glass autoclave, which was pressurized with CO (5 atm) and then heated for 2 h at 80 °C with stirring. After cooling and removal of the volatiles, the residue was subjected to TLC separation (silica; eluted with CH_2Cl_2:hexanes = 1:10). Recrystallization of the yellow fraction from hot hexanes afforded **12a** (14.9 mg, 0.027 mmol, 93% yield) as yellow crystals. Anal. Calcd for $C_{17}H_{20}O_3SiRu_2$: C, 40.63; H, 3.98. Found: C, 40.51; H, 3.89. The reaction of **6e** was carried out in the same method. **12b** (98% yield, yellow crystals): Anal. Calcd for $C_{32}H_{26}O_3SiRu_2$: C, 55.81; H, 3.78. Found: C, 55.62; H, 3.65.

Thermolysis of 6a,e in the Presence of PPh_3. A benzene solution (1 mL) of **6a** (23.4 mg, 0.043 mmol) and PPh_3 (34.0 mg, 0.13 mmol) was heated for 2 h at 80 °C with stirring. After cooling and removal of the volatiles, the residue was subjected to TLC separation (silica; eluted with ether:hexanes = 1:7). Recrystallization of the yellow fraction from toluene−hexanes afforded **13a** (40.0 mg, 0.031 mmol, 74% yield) as yellow crystals. Anal. Calcd for $C_{34}H_{35}O_2PSiRu_2$: C, 55.43; H, 4.75. Found: C, 55.87; H, 4.33. The reaction of **6e** was carried out in the same method. **13b** (92% yield, yellow crystals): Anal. Calcd for $C_{49}H_{41}O_2PSiRu_2$: C, 63.77; H, 4.45. Found: C, 64.00; H, 4.71.

Reaction of $Cp_2Ru_2(\mu$-$CHSiMe_3)(\mu$-$CO)(CO)(MeCN)$ (17) with $HSiMe_3$. An acetonitrile solution (150 mL) of **12a** (30 mg, 0.06 mmol) was photolyzed by a high-pressure mercury lamp (Ushio UM-452) for 6 h.[5j] After consumption of **12a** was confirmed by IR, the volatiles were removed under reduced pressure and the residue was washed with ether. Though an analytically pure sample of **17** was not obtained, it was characterized spectroscopically: ^{1}H-NMR (CD_3CN) δ_H 7.18 (1H, s, μ-CH), 5.09, 4.72 (5H × 2, s × 2, Cp_2), 0.12 (9H, s, $SiMe_3$); IR (CH_3CN) ν(C≡O) 1915, 1750 cm^{-1}. Addition of 3 equiv of $HSiMe_3$ to a C_6D_6 solution of **17** produced **6a** immediately as observed by ^{1}H-NMR.

Formation of Stannylated μ-Methylene Compounds 20 and 21a,b. The reaction was carried out in essentially the same manner as described for the Si analogues (**6**) with use of hydrostannanes in place of hydrosilanes. The hydrido−stannyl−μ-methylene species **20** was formed quantitatively as observed by the reaction conducted in C_6D_6. Compounds **20**

Table 5. Crystallographic Data for 6d, 6e·hexane, 12a, 13a, 21a, and 22

complex	**6d**	**6e**·hexane	**12a**	**13a**	**21a**	**22**
formula	$C_{29}H_{34}O_2Si_2Ru_2$	$C_{51}H_{56}O_2Si_2Ru_2$	$C_{17}H_{20}O_3SiRu_2$	$C_{34}H_{35}O_2SiPRu_2$	$C_{19}H_{30}O_2Sn_2Ru_2$	$C_{31}H_{28}O_2SnRu_2$
fw	672.9	1007.4	502.6	736.9	730.0	753.4
space group	$P2_12_12_1$	$P2_1/a$	$P2_1/m$	$P\bar{1}$	$P2_1$	$P2_1/c$
a/Å	12.504(1)	19.337(2)	6.936(2)	11.407(5)	8.387(2)	10.724(1)
b/Å	23.643(3)	17.656(2)	14.947(2)	14.631(5)	10.144(2)	13.220(2)
c/Å	9.551(2)	14.023(2)	9.520(4)	9.750(2)	14.273(4)	19.802(2)
α/deg				100.80(2)		
β/deg		92.310(8)	95.12(2)	98.41(1)	109.58(2)	98.42(3)
γ/deg				78.60(3)		
V/Å^3	2823.6(7)	4784(1)	929.9(5)	1556.7(10)	1209.4(5)	2777.1(6)
Z	4	4	2	2	2	4
d_{calcd}/g·cm^{-3}	1.58	1.40	1.80	1.57	2.00	1.80
μ/cm^{-1}	11.6	7.2	16.7	10.9	32.6	19.9
2θ/deg	5−55	2−45	5−60	5−50	5−55	5−50
no. of data collcd	3687	7323	3021	5794	3133	5419
no of unique data with I > 3σ(I)	3013	4754	2073	4090	2225	2407
no. of params refined	324	528	115	365	225	325
R	0.030	0.043	0.036	0.041	0.041	0.056
R_w	0.026	0.043	0.035	0.043	0.035	0.040

were not obtained analytically pure and were characterized by means of spectroscopy (see Table 1). Isolated yields and analytical data of **21** are as follows. **21a** (52% yield, yellow solid): Anal. Calcd for $C_{19}H_{30}O_2Sn_2Ru_2$: C, 31.26; H, 4.11. Found: C, 31.20; H, 4.95. **21b** (47% yield, yellow solid): Anal. Calcd for $C_{37}H_{66}O_2Sn_2Ru_2$: C, 45.21; H, 6.72. Found: C, 45.48; H, 7.01.

Low-Temperature Reaction of 4-d_2 with $HSnMe_3$. The low-temperature reaction of **4**-d_2 with $HSnMe_3$ was carried out as described for the low-temperature reaction of **4** with $DSiMe_2Ph$ (see above).

Reaction of 4 with $HSnPh_3$. The MeCN complex **4** (75.0 mg, 0.17 mmol) and $HSnPh_3$ (300 mg, 0.85 mmol) were allowed to react in benzene (2.5 mL) for 24 h at rt. After removal of the volatiles under reduced pressure the residue was subjected to preparative TLC separation (eluted with CH_2Cl_2:hexanes = 4:1). The mononuclear stannyl complex **24** (27.2 mg, 0.047 mmol, 14% yield) was identified by comparison of NMR and IR data with those of reported data.[25] **22** (58.6 mg, 0.078 mmol, 46% yield): ^{1}H-NMR ($CDCl_3$) δ_H 7.62−7.16 (m, Ph), 5.31, 5.02 (5H × 2, s × 2, Cp_2), 0.38 (s, $^2J_{Sn-H}$ = 43 Hz, SnMe); see also Chart 1. ^{13}C-NMR ($CDCl_3$): δ_C CO signals, 205.2, 202.0 (s × 2, CO); Ph signals, 150.4 (d, J = 162 Hz), 146.2 (s, ipso), 146.1 (s, ipso), 143.3 (d, J = 160 Hz), 136.3 (J = 156 Hz), 136.2 (d, J = 156 Hz), 127.7 (d, J = 160 Hz), 127.5 (d, J = 160 Hz), 127.4 (d, J = 161 Hz), 127.3 (d, J = 161 Hz), for the bridging Ph signals, see Chart 1; Cp signals, 86.0 (d, J = 178 Hz), 82.9 (d, J = 178 Hz); SnMe, −5.8 (q, J = 128 Hz). IR (CH_2Cl_2): ν(C≡O) 1906 cm^{-1}. Anal. Calcd for $C_{31}H_{28}O_2Ru_2Sn$: C, 48.42; H, 3.72. Found: C, 48.21; H, 3.91. **23** (12.7 mg, 0.013 mmol, 8% yield): ^{1}H-NMR ($CDCl_3$) δ_H 7.83−6.95 (20H, m, Ph), 4.81 (10H, s, Cp_2). ^{13}C-NMR ($CDCl_3$): δ_C 200.7 (CO), 153.0 (s, ipso), 135.6 (d, J = 161 Hz, Ph), 135.4 (d, J = 159 Hz, Ph), 127.2 (d, J = 166 Hz, Ph), 79.3 (d, J = 180 Hz, Cp). IR (CH_2Cl_2): ν(C≡O) 1908 cm^{-1}. Anal. Calcd for $C_{36}H_{30}O_2Sn_2Ru_2$: C, 46.28; H, 3.22. Found: C, 46.02; H, 3.40.

Reaction of 6a with H_2. A glass autoclave containing a C_6D_6 solution (0.50 mL) of **6a** (15.2 mg, 0.028 mmol) was cooled in a dry ice bath and then evacuated. After being filled with hydrogen gas (1 atm), it was closed and placed in a GLC oven (at 65 °C). After 2 h propane (20 μL; internal standard) was added through a rubber septum and then the yield of methane was determined by GLC. The organometallic products were analyzed by ^{1}H-NMR.

Reaction of 5a with H_2. A sample of **5a** was prepared by the reaction of **4** (21.3 mg, 0.048 mmol) with $HSiMe_3$ (10 μL, 0.12 mmol) in benzene (2 mL) for 5 min (see above). After removal of the volatiles C_6D_6 (0.30 mL) was added and the resulting solution was transferred to a thick-walled NMR tube, and the tube was closed with a screw cap. Then hydrogen was introduced as described above. After stirring of the mixture for 15 h at rt propane (50 μL; internal standard) was added through a rubber septum and then the yield of methane was determined by GLC.

Single-Crystal X-ray Crystallography. Single crystals of **6d**, **6e**·hexane, **21a**, **22**, **12a**, and **13a** were obtained by recrystallization from CH_2Cl_2−hexanes. Suitable crystals were mounted on glass fibers. Diffraction measurements were made on a Rigaku AFC-5R automated four-circle diffractometer by using graphite-monochromated Mo Kα radiation (λ = 0.710 59 Å). The unit cells were determined and refined by a least-squares method using 20 independent reflections (2θ ∼ 20°). Data were collected with an ω−2θ scan technique. If $\sigma(F)/F$ was more than 0.1, a scan was repeated up to three times and the results were added to the first scan. Three standard reflections were monitored at every 150 measurements. The data processing was performed on a micro Vax II computer (data collection) and an IRIS Indigo computer (structure analysis) by using the teXsan structure solving program system obtained from the Rigaku Corp., Tokyo, Japan. Neutral scattering factors were obtained from the standard source.[35] In the reduction of data, Lorentz and polarization corrections and an empirical absorption correction (ψ scan) were made. The crystallographic data and the results of analyses are summarized in Table 5.

The structures were solved by a combination of the direct methods and Fourier synthesis (SAPI91 and DIRDIF). All the non-hydrogen atoms except the hexane carbon atoms in **6e**·hexane were refined anisotropically. The μ-CH_2 and μ-$CHSiMe_3$ hydrogen atoms except those of **21a** were located by examination of the difference Fourier maps and were refined isotropically. The remaining hydrogen atoms were fixed at the calculated positions (C−H = 0.95 Å) and were not refined.

Acknowledgment. Financial support from the Ministry of Education, Science, Sports, and Culture of the Japanese Government (Grants-in-Aid for Scientific Research on Priority Area, No. 05236103; Grant-in-Aid for Scientific Research, No. 07651048) is gratefully acknowledged. R.H. thanks the Tsuji Asia Scholarship Foundation for the generous support.

Supporting Information Available: Tables of positional parameters and B_{eq} values, anisotropic thermal parameters, and bond lengths and angles for the structures and figures showing the atomic numbering schemes of **6e**·hexane (25 pages). Ordering information is given on any current masthead page.

OM960258R

(35) *International Tables for X-Ray Crystallography*; Kynoch Press: Birmingham, U.K., 1975; Vol. 4.